Journal of Hydrology: Regional Studies 9 (2017) 163–182

Contents lists available at ScienceDirect

Journal of Hydrology: Regional Studies

journal homepage: www.elsevier.com/locate/ejrh

Temporal changes in groundwater quality of the Saloum coastal aquifer

Ndeye Maguette Dieng[a,c,*], Philippe Orban[a], Joel Otten[a], Christine Stumpp[b], Serigne Faye[c], Alain Dassargues[a]

[a] Hydrogeology & Environmental Geology – Dpt ArGEnCo, Aquapole, University of Liège, 4000 Liège, Belgium
[b] Institute of Groundwater Ecology, Helmholtz Zentrum München, Ingolstädter Landstrasse 1, D-85764 Neuherberg, Germany
[c] Department of Geology – FST, University of Cheikh Anta Diop, Dakar, Senegal

ARTICLE INFO

Article history:
Received 27 April 2016
Received in revised form 7 December 2016
Accepted 10 December 2016

Keywords:
Groundwater salinization
Self organizing maps
Geochemical processes
Environmental isotopes
Saloum inverse estuary

ABSTRACT

Study region: Groundwater in the southern part of the Saloum Basin in Senegal.
Study focus: The Saloum estuary is a hypersaline and 'inverse' estuary where the salinity of river water increases in the upstream direction. This region is problematic in that due to the underlain superficial Continental Terminal aquifer bordered by the hypersaline estuary constitutes the unique fresh groundwater reservoir for water supply for its estimated 466,000 residents living in 18 rural districts (belonging to the regions of Fatick, Kaolack and Kaffrine). This is of high value given that the deep Maastrichtian aquifer (200–300 m depth) is saline. This study aims to describe and understand temporal changes in the chemical and isotopic compositions of groundwater, the geochemical processes and especially the groundwater salinization.
New hydrological insights for the region: The analytical data were discriminated into 3 groups on the basis of the water types. Na-Cl, Ca-Cl and Ca-SO_4 rich waters derived from saline water intrusion at the vicinity of the Saloum River accompanied by ion exchange reactions and pollution dominate the first group. The second group located mainly in the centre and eastern parts of the region is featured fresh groundwater of Ca-HCO_3 derived from calcite dissolution reactions. The third group of Na-HCO_3 type and less mineralized indicates freshening processes by recently infiltrating rainwaters. Slight seasonal chemical variations are observed due to new infiltrating water reaching the water table.

High variation in rainfall between the 2 reference years (2003 and 2012) also changes chemical patterns in the groundwater. Chemical evolution of the groundwater is geographically observed and is due to a combination of dilution by recharge, anthropic contamination and seawater intrusion. The results of environmental isotopes ($\delta^{18}O$, $\delta^{2}H$) compared with the local meteoric line indicate that the groundwater has been affected by evaporation processes before and during infiltration. The results also clearly indicate mixing with saltwater and an evolution towards relative freshening between 2003 and 2012 in some wells near the Saloum River.

* Corresponding author at: Department of Geology – FST, University of Cheikh Anta Diop, Dakar, Senegal and Hydrogeology & Environmental Geology – Dpt ArGEnCo, Aquapole, University of Liège, 4000, Liège, Belgium..
E-mail addresses: nmdieng@doct.ulg.ac.be, ndeye81.dieng@ucad.edu.sn, diengmaguette@yahoo.fr, mdmaguettedieng@gmail.com (N.M. Dieng).

http://dx.doi.org/10.1016/j.ejrh.2016.12.082

Introduction

The Continental Terminal (CT) aquifer is a unique freshwater reservoir, which supports various water needs in the Saloum region located mid-West of Senegal. Unfortunately, this resource is threatened by saltwater intrusion derived from both the ocean in the western part and from the hypersaline Saloum River which limits the system in the northern part. The Saloum hydrologic system is a tide-influenced inverse estuary in which high evaporation rates combined with low flow in this context of flat topography result in salt deposition and high salinity of the surface water body. As defined by Pritchard (1967), in inverse or hypersaline estuary systems, the salinity of the river water substantially exceeds seawater salinity. This pattern is governed by the net loss of fresh water usually resulting from an excess of evaporation over runoff and precipitation. These systems, for which salinity increases upstream from the river mouth towards inland regions, occur mostly in arid or semi-arid parts of the world (Largier et al., 1997), such as Australia (Wolanski, 1986) and West Africa (Barusseau et al., 1985; Diop, 1986; Page and Citeau, 1990; Savenije and Pagès, 1992; Ridd and Stieglitz 2002; Mikhailov and Isupova, 2008). Therefore, groundwater salinization in these areas is closely linked to direct saltwater intrusion and high evaporation. Previous studies in Australia evidenced groundwater contamination processes through estuarine saltwater intrusion in the Swan-Canning Estuary (Smith and Turner, 2001) and in the Pioneer Valley, Northern Queensland (Werner and Lockington, 2004). In the Saloum region, Noël (1975) then Diluca (1976) investigated the geometry, flow regime, and chemical characteristics of groundwater in the CT aquifer. Salinity pattern and associated geochemical processes using basic ion chemistry were described by Faye et al. (2001, 2003, 2004, 2009, 2010). The results pointed out that the groundwater resource is constrained by the occurrence of moderate to high salinity in the northern (near the Saloum River) and western (coastal area) parts of the aquifer. There, many shallow wells have been impacted by the occurrence of saline water. Further investigations were done by Faye et al. (2004) using minor elements (B, Br, Sr) and isotopic indicators together with some major ions for constraining source, and relative age and sorption/desorption reactions related to refreshening and salinization processes. In this latter study, boron concentrations (7–650 μg/L) were tested against the binary mixing model. Results showed salinization processes are evidenced by B sorption and Na depletion when the Saloum River water intrudes the aquifer (salinization) in the northern part of the region. Conversely, B desorption and Na enrichment occur as the fresh groundwater flushing displaces the saline groundwaters in the coastal strip (refreshening). In the central zone where ancient intrusion prevailed, the process of freshening of the saline groundwater was indicated by the changes in major ion chemistry as well as B desorption and Na enrichment. The relatively stable isotope and tritium contents of the CT aquifer indicated that groundwater is derived from recent precipitation and mixing with recently infiltrating waters and evaporation contribute to the changes in isotopic signature.

Therefore, salinisation constitutes a major issue in the Saloum region due to the fact that potable drinking water needs rely solely on the CT groundwater resource given that the deep Maastrichtian aquifer (200–300 m) exhibits high chloride contents (500–1000 mg/L) and some hazardous elements, such as fluoride and boron, which reach concentrations of 2–4 and 1–2 mg/L, respectively (Travi, 1988). Therefore, the CT aquifer represents a unique accessible freshwater resource in the region.

Despite of these valuable results, temporal (both seasonal and long term) effects were not adressed. Therefore, the present study aims at reassessing the groundwater quality changes of the CT aquifer in the light of the new constraints (e.g. changes in climatic conditions and pumping constraints), and the new groundwater flow pattern configuration. Specifically, this study intends to: (1) identify seasonal variations in the chemical patterns in relation to geochemical reactions and dilution using statistical tools, such as Self Organizing Maps (SOMs), and (2) assess the temporal trend of groundwater chemistry and salinization using chemical and isotopic groundwater compositions.

2. Study area

2.1. Location and geomorphology

The study area is located in the western part of Senegal and covers the southern part of the Saloum hydrologic Basin except for the mangrove system. The surface area is approximately 3380 km^2 (Fig. 1) and is limited to the North by the Saloum River, to the West by the mangrove area and to the South and East by the Gambia River catchment.

The geomorphologic setting which consists of a gently sloping plain that extends toward the coast is incised by a network of depressions where temporary streams drain run-off water during the rainy season. A digital elevation model (±4 m precision) that was created from topographical maps (1:50,000) and measured points shows elevations ranging from −1 m in the West and the North (near the mangroves and the Saloum River) to +50 m in the South and East towards the plateau zone bordered by the Gambian Basin (Fig. 1). In the northern and western regions along the Saloum River and the coast, respectively, a succession of high areas (10–30 m) and depressions (0–10 m) forms the landscape.

Land use/land cover of the study area were investigated using October 2010 Landsat image (ETM) and linear discriminant classifier (LDC) supervised classification method (Dieng et al., 2014). Surface features generated comprise rainfed agricultural crops (52%), natural vegetation (40%) (composed of savannah, wooded park, bushland and shrub steppe trees), dispersed habitations predominantly villages (3.5%), salty barren soils locally called “tanne” (2%), surface water bodies (1.5%) and mangrove ecosystem areas (1%).

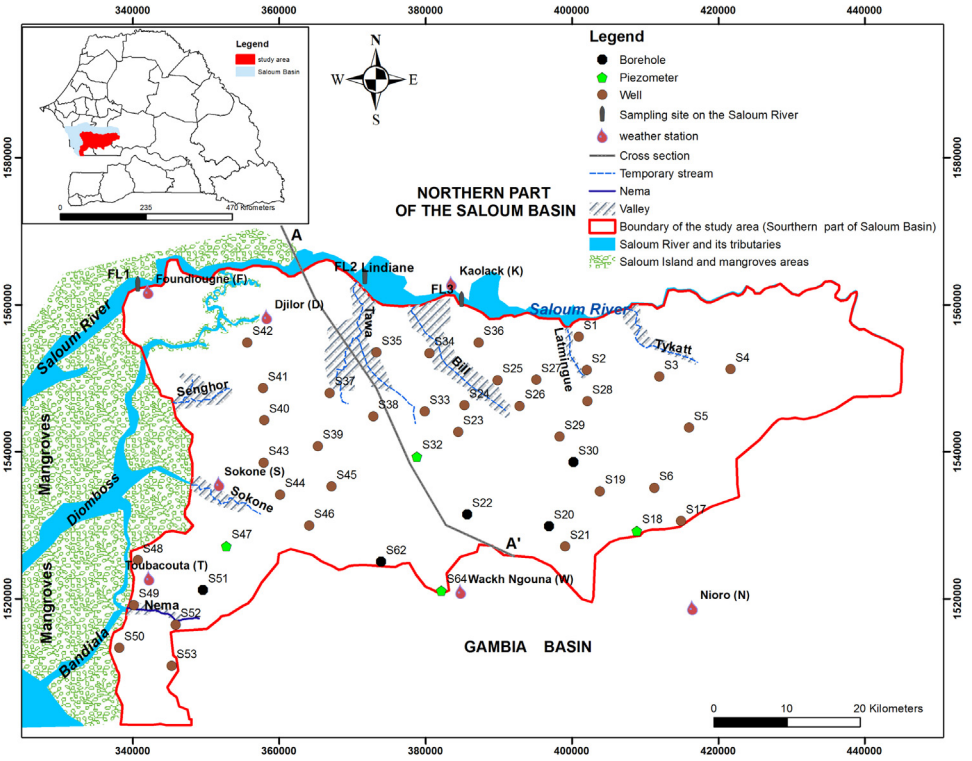

Fig. 1. Location of the investigated area and monitoring network. The dark line indicates the location of the cross-section A-A' presented in Fig. 2.

2.2. Climate

The climate of the region is tropical with two distinct seasons: a dry season from November to May and a rainy season from June to October. The average annual rainfall from 1960 to 2012 varied from 750 mm in the southern part of the basin at Nioro station to 615 mm in the northern part at Kaolack station with a South-North decreasing gradient. The rainfall record (Fig. 3) at Kaolack station compared to the mean reference 1960–1990 shows a humid period from 1928 to 1971 followed by a dryer period from 1971 to the end of the 1990s, which occurred through most of the Sahel zone. In some Sub-Saharan countries, such as the study area, this dry period was followed by progressively wetter years (Lebel and Ali, 2009).

Available climatic data (i.e., precipitation, temperature, relative humidity, insulation, and wind speed) for the period from 1981 to 2012 collected from the Senegal National Meteorological Agency at the Kaolack and Nioro weather stations show that the average annual temperature ranges from 28 to 29 °C. The average annual potential and actual evapotranspiration values calculated using the Penman method (Allen et al., 1998) are 2030 and 552 mm/yr respectively.

2.3. Hydrology

The hydrologic system of the region is mainly composed by the Saloum River and its two tributaries, the Bandiala and Diomboss rRivers. The Nema River, which is the only perennial freshwater stream, flows towards the Bandiala River (Fig. 1). It receives a groundwater base flow of between 0.012 and 0.03 m^3/s during the dry and rainy seasons, respectively (Ngom, 2000). Downstream these rivers and streams, small seawater creeks locally called "bolons" occur in addition to the large low-lying estuary bearing tidal wetlands, and the mangrove ecosystem. As discussed previously, the Saloum estuary is an inverse estuary. Measurements data during the dry season showed that the salinity of the Saloum River increases from 36.7 g/L at the mouth to more than 90 g/l at Kaolack (located 120 km from the mouth) (Diop, 1986). Page and Citeau (1990) using data record revealed that salinity of the Saloum River is highly sensitive to climate variations with a gradient of approximately 1.3 g/l per year between 1950 and 1986 (Fig. 3). This observation is in accordance with works of Savenije and Pagès (1992) in western African inverse estuaries which evidenced sharp increase in salinity gradients during the Sahel droughts in the 1960s.

2.4. Geological and hydrogeological context

The study area belongs to the Senegalese-Mauritanian sedimentary basin, which is the largest coastal basin in northwest Africa and bears formations from the Cretaceous to the Quaternary (Bellion, 1987). The geological context of the region

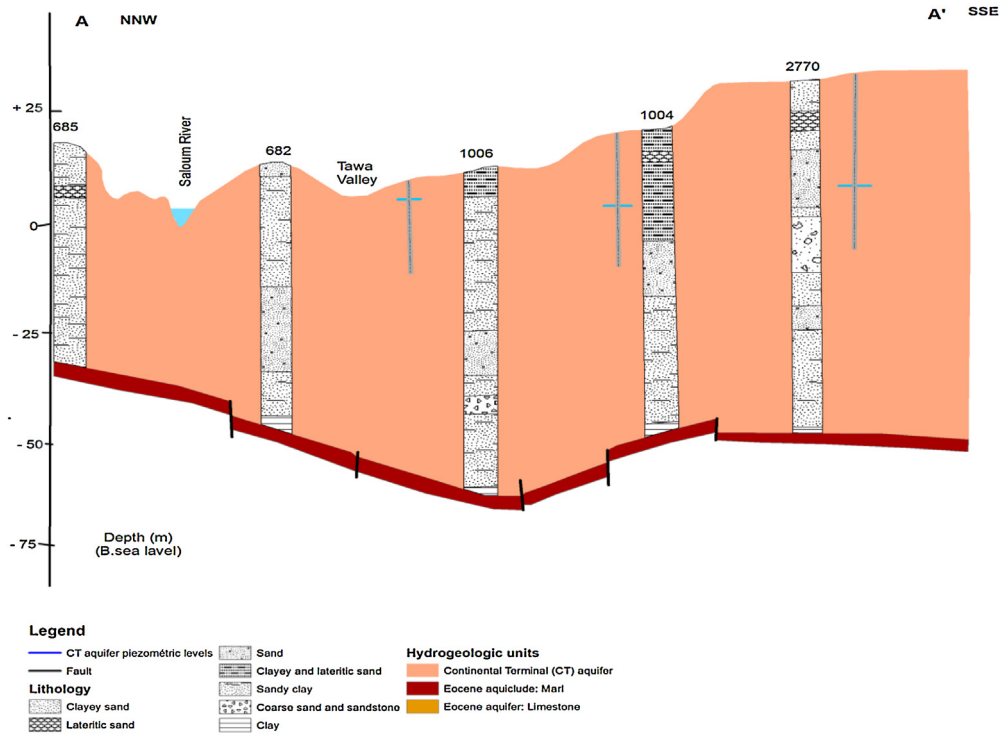

Fig. 2. Cross section of the study area showing the geological formation and the piezometric level of CT groundwater (cross section indicated in Fig. 1).

has been studied using lithological information from boreholes and hand-dug wells in addition to regional previous studies (Lappartient, 1985; Le Priol and Dieng, 1985) and a recent regional geological map (1:500 000) (Roger et al., 2009). The CT formations, which are the focus of this study, are present throughout the region and are covered by a thin and younger Quaternary sand layer and locally by alluvial deposits in the river plains. These formations overlie the impervious marl/clay Eocene formations.

The CT sediments are detrital marine Cenozoic (Oligo-Miocene to Pliocene) origin and show evidence of intense ferralitic alteration during the late Miocene, including ferruginous concretions (Lappartient, 1985; Conrad and Lappartient, 1987). They are laterally and vertically heterogeneous and contain discontinuous interbedded sandstone, sandy clay, clayey sand, silt and clay (Noël, 1975; Lappartient, 1985; Conrad and Lappartient, 1987) (Fig. 2). Locally, clay sandstone beds and ferruginous crusts are present at the top of the formations. Kaolinite forms the cement in the non-ferruginous sandstone and sand sediments and represents the dominant clay mineral. Goethite is predominant and forms the cement of the quartz grains in the ferruginous sandstone horizon. Trace quantities of illite have been identified while in the eastern part of the region, the quartz grains are coated by calcite (Lappartient, 1985).

Hydrogeologically, the CT formations are considered as unconfined aquifer which thickness increases from NNW (less than 50 m) to SSE (approximately 100 m) and from West (less than 50 m) to East (approximately 100 m) (Fig. 2). The aquifer reservoir lies on an irregular and impervious Eocene substrate composed of marl and limestone covered by clay (Fig. 2) (Ly and Aglanda, 1991; Sarr, 1995). The hydraulic conductivity and storage coefficient values obtained from pumping test data under depth averaged conditions range from 0.5 to 8.6×10^{-4} m/s and from 0.5 to 21×10^{-2}, respectively (Diluca, 1976). Thirty-one boreholes with pumping rates between 10 and 45 m^3/h and numerous traditional wells are used for the water supply in this region and total withdrawal is estimated at 8000 m^3/day. Groundwater recharge occurs mainly through rainwater infiltration. Computed values using chloride mass balance (CMB) method (chloride profiles at different sites obtained during the course of this study and not shown here) in the unsaturated zone, and hydrological budget (ETo computed by Penman formula) are variable and range from 17 to 100 mm/year and from 19 to 130 mm/year, respectively. These recharge values are similar to those obtained by Edmunds and Gaye (1994) (11–108 mm/year) using the same CMB method. The spatial variability is likely to be due to local variations in soil type and texture (notably clay contents) and to vegetation cover. The CMB approach uncertainties in our context can be linked to potential Cl contribution from other sources such as salt water intrusion or anthropogenic input. Water table measurements were obtained during the 2012 campaigns in May (end of dry season) and in November (end of rainy season). They were converted to head values through an accurate DGPS topographic survey of the sampling sites. It allows to reassess groundwater flow patterns shown in Fig. 4 for the dry season. A similar flow pattern is obtained for the rainy season (not shown here). Head (h) distribution features three groundwater mounds located in the northwest ($9.8 \leq h \leq 11.7$ m), in the southwest along the upstream part of the Nema River ($25.3 \leq h \leq 26.6$ m), and in the North ($13.2 \leq h \leq 16$ m). A marked depression is observed North and parallel to the Saloum River, where the measured

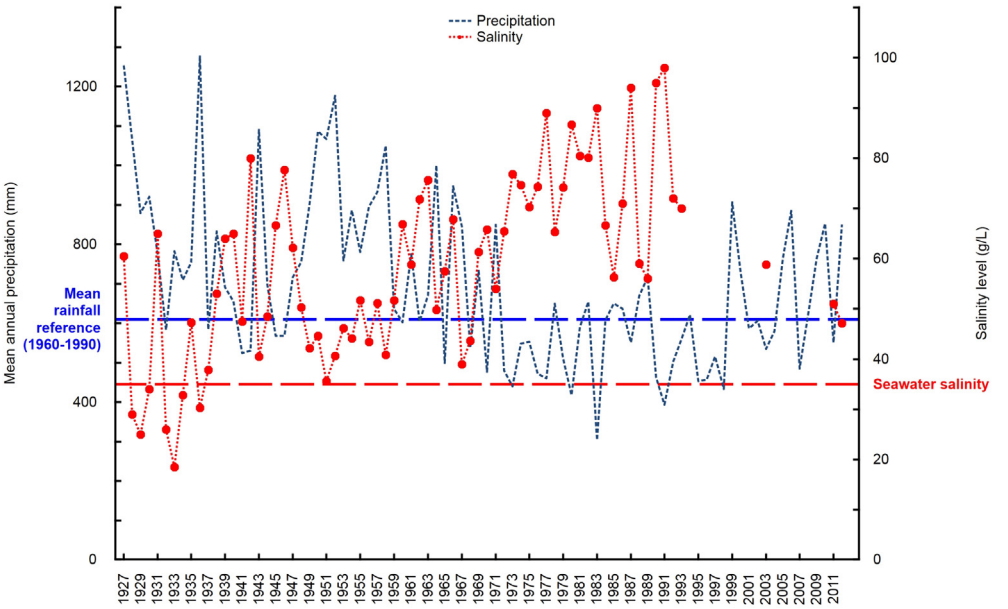

Fig. 3. Interannual variation of the Saloum River salinity (in red) and of the mean annual rainfall measured at Kaolack locality from 1927 to 2012 modified from Page and Citeau (1990).

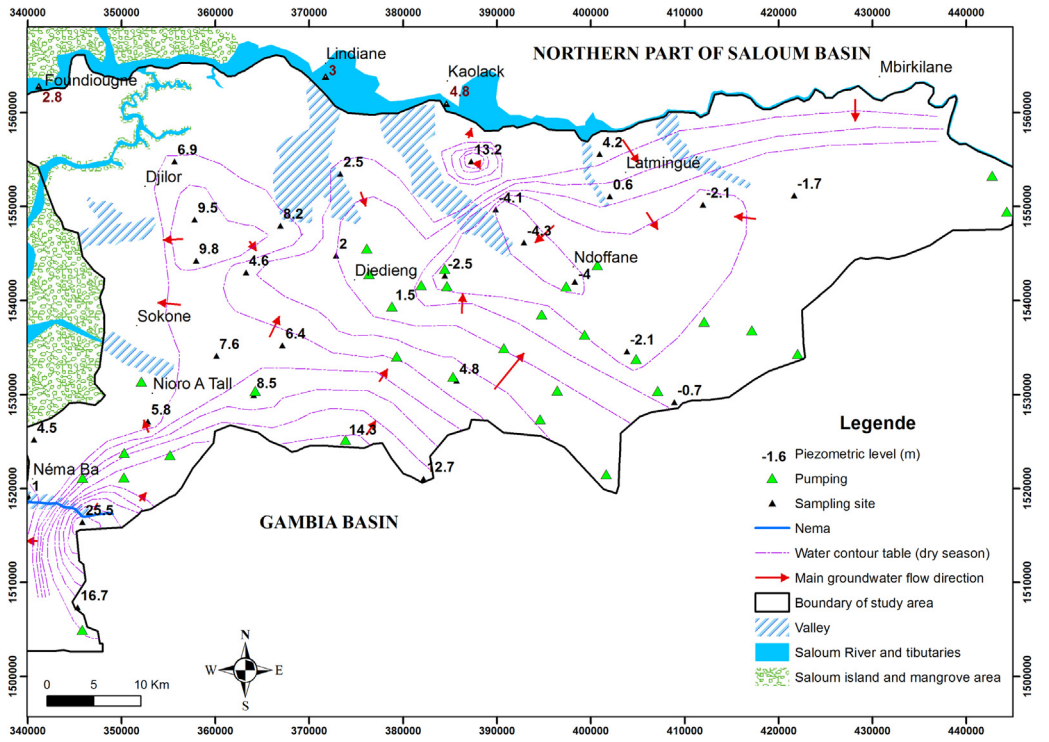

Fig. 4. Groundwater piezometric map in the CT aquifer during the dry season of 2012.

heads are below mean sea level (as low as −4 m). This latter depression is a common feature in many unconfined aquifers in sub-Saharan Africa, such as in Trarza/Mauritania, in Yaere/North Cameroon, in Gondo, Nara, and Azaouad/Mali, and in Kadzell/Niger (Archambault, 1960; Degallier, 1962; Aranyossy et al., 1989; Ndiaye et al., 1993; Favreau et al., 2002; Ngounou Ngatcha et al., 2007; Koussoube, 2010). Isotopic studies performed in Mali (Aranyossy et al., 1989), Niger (Favreau et al., 2002) and Senegal (Ndiaye et al., 1993) suggest that the combined effects of high evapotranspiration and low horizontal permeability are the main causes of this type of piezometric depressions since pumping rates in these area are low.

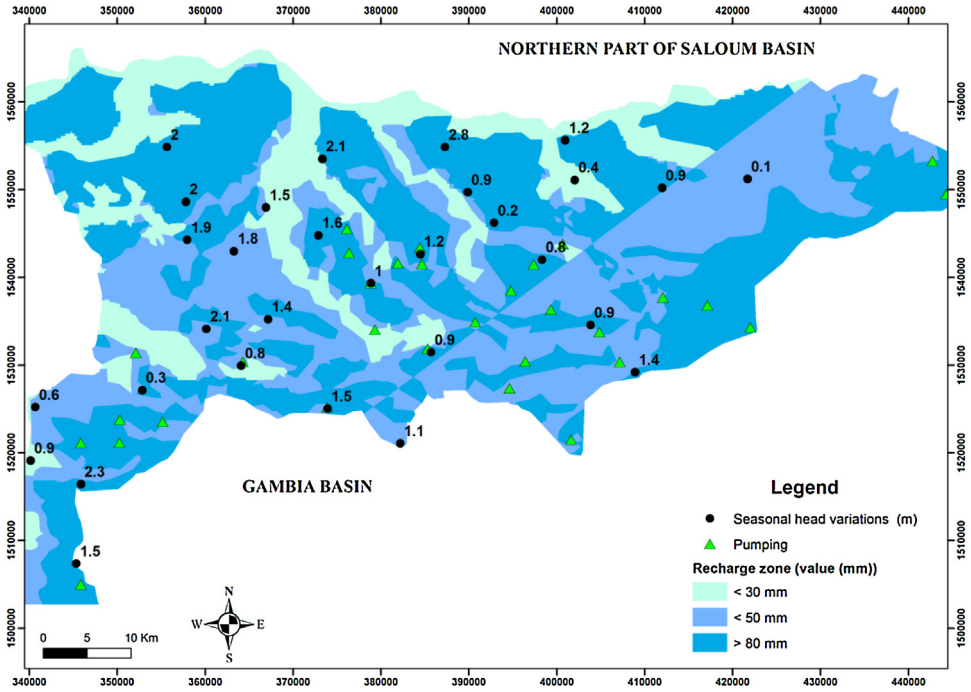

Fig. 5. Recharge map and punctual observed seasonal changes in piezometric heads.

Based on this configuration, several groundwater flow patterns can be depicted:

– from the northwest and northern mounds towards the sea and the Saloum River, where the head values decrease near the shore but are still positive;

– from the southwest mound in all directions; occurrence of the groundwater mound in the zone sustains the Nema River flow during low stage period (Ngom, 2000);

– from the Saloum River and the southern mound to the piezometric depression.

The seasonal and long term head variations obtained from 2012 (dry and rainy season) and 1973 datasets may reflect seasonal recharge and interannual evolution, respectively. Seasonal head variations recorded in 2012 range from 0.1 to 2.8 m with the highest value located far from the pumping area in a zone of relative high recharge (> 50 mm). The lowest value of head variation is observed near the pumping area in a zone of relative low recharge (<30 m) (Fig. 5).

Comparison of the 2012 head values with heads measured during pre-development and driest period of 1973 in few reference points show water table rise from 0.7 to 6.8 m (mean 4.2 m) (Fig. 6). This is observed despite the pumping from more than 100 boreholes and numerous dug wells since the early 70s. This long term water table rise probably reflects sensitivity of the system to climate and especially to annual rainfall (440 and 847 mm respectively in 1973 and 2012).

3. Materials and methods

3.1. Field campaigns and laboratory protocols

To complete the existing dataset (including the data acquired in 2003), two field campaigns were conducted in May 2012 (end of the dry season) and November 2012 (end of the rainy season). The measured and sampled network comprises forty-four groundwater sampling points (composed of 5 boreholes, 35 hand-dug wells and 4 piezometers) in addition to three surface water sampling sites along the Saloum River (at Foundiougne (FL1), Lindiane (FL2) and Kaolack (FL3)) (Fig. 1). Prior to sampling, depth to water table and physico chemical parameters such as pH, electrical conductivity (EC) and temperature (T) were measured in the field at each site using a multi-parameter probe. The groundwater samples were collected after purging the piezometers while wells and boreholes used for water supply did not need to be purged because they were pumped continuously.

For chemical analyses, a set of two samples was collected for each point and subsequently filtered through 0.45 μm membranes into polyethylene bottles. One acidified to a pH less than 2 using high purity HNO_3 for cation analysis, and the other one not acidified for anion analysis.

For stable isotope analyses of oxygen (^{18}O) and hydrogen (^{2}H), selected points of the network and the three Saloum River points were sampled during the wet season and tightly sealed in 1-l polyethylene bottles without filtered.

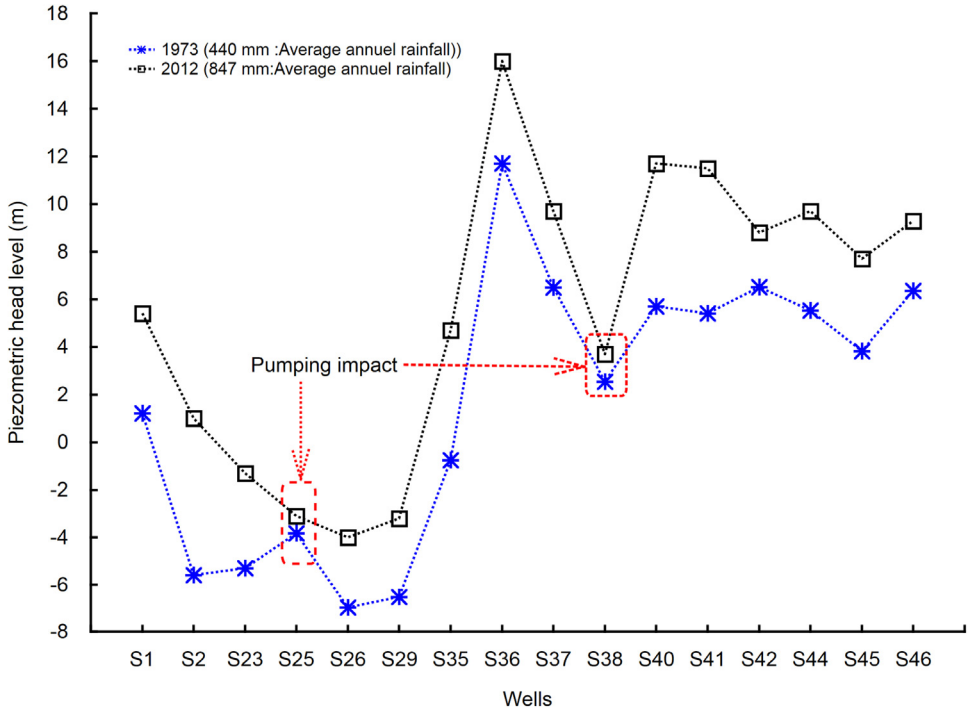

Fig. 6. Differences between piezometric levels measured in November 1973 and November 2012 in 16 wells.

Records of measured quantity of rain and 2012 rainwater samples were collected from 7 climatic stations, namely Kaolack (K), Nioro (N), Wakh Ngouna (W), Foundiougne (F), Djilor (D), Sokone (S) and Toubacouta (T).

The chemical analyses for major ions (Ca^{2+}, Na^{+}, Mg^{2+}, K^{+}, Cl^{-}, HCO_3^{-}, SO_4^{2-} and NO_3^{-}) were performed using standard methods of flame atomic absorption, potentiometric, and titration at the Liege University Hydrogeology Laboratory (Belgium). The Environmental isotope analyses were performed at the Helmholtz Zentrum München, Institute of Groundwater Ecology (Neuherberg/Germany) using dual-inlet mass spectrometry (Coplen, 1988) and results are expressed in the conventional δ-per mil (δ ‰) notation with reference to the Vienna Standard Mean Oceanic Water (VSMOW) with precisions of ±0.1‰ for $\delta^{18}O$ and ±1‰ for $\delta\ ^{2}H$.

3.2. Data analysis and multivariate statistical analysis

While the electrical conductivity (EC) is routinely used to measure the mineralisation of water, conventional methods involving major and minor ions analysis, ionic ratios, and isotopic methods are used in assessing groundwater quality (Ghesquière et al., 2015; Nicolini et al., 2016) and the interaction between freshwater and saline water (Magaritz et al., 1981; Mercado, 1985; Kim et al., 2003).

Multivariate analysis methods, such as Factor Analysis (FA), Principal Component Analysis (PCA) and Hierarchical Classification Analysis (HCA), are also often used to identify major groundwater groups and factors that affect the groundwater chemistry in aquifers (Mudry, 1991; Güler et al., 2002; Belkhiri et al., 2012; Gamble and Babbar-Sebens, 2012; Montcoudiol et al., 2015; Ghesquière et al., 2015; Ibrahima et al., 2015). However, these multivariate analyses are generally based on linear principles (Mudry, 1991; Gamble and Babbar-Sebens, 2012) and cannot overcome difficulties arising from biases due to complexity and non-linearity in datasets and from the inherent correlations between variables. The SOMs method (Kohonen, 1982) applied here is an alternative to these latter methods to efficiently deal with datasets that are ruled by complex, non-linear relationships in the analysis and diagnosis of dynamic systems (Hong and Rosen, 2001; Hong et al., 2004; Garcia and Shigidi, 2006; Peeters et al., 2007; Gamble and Babbar-Sebens, 2012; Gning, 2015). It allows clustering a set of hydrochemical data into two or more independent groups (Kohonen, 1995;). This method outperforms the other statistical tools in that it can successfully: 1) deal with the nonlinearities of the system; 2) be developed from data without requiring mechanistic knowledge of the system; 3) handle noisy or irregular data and be easily and quickly updated; and 4) interpret and visualize information from multiple variables or parameters (Kohonen, 2001).

The component planes and U-matrix are visualization maps that use a hexagonal topology to represent the main output results. The component planes show high and low values on a standardized map to identify correlations between different parameters. Ultimately, in the SOMs analysis, all these component maps are combined to create a unified matrix (U-matrix) that characterizes the Euclidean distances between each node (Peeters et al., 2007; Gamble and Babbar-Sebens, 2012). The

clustering is based on a visual inspection of the U-matrix where clusters correspond to different types of groundwater with respect to the contribution of each element. The information obtained from SOMs application can then be used to highlight water mineralization processes that occur in the aquifer based on the degree of salinity and the spatiotemporal hydrogeochemical variability.

In this study, 11 chemical variables (EC, pCO_2,pH, Ca^{2+}, Mg^{2+}, Na^+, K^+, Cl^-, HCO_3^-, $SO_4^{2-}$and NO_3^-) are processed using the SOMs Toolbox of the MATLAB™ code to first investigate the variables that affect the salinity and their relationships. Classical tools, such as Piper diagrams and bivariate analysis, are then used to confirm the relationships between the variables.

4. Results and discussion

4.1. Hydrochemical characteristics

The results from the in-situ physico-chemical surveys and the chemical and isotopes analyses of groundwater, surface water, and seawater samples are presented in Table 1, and the mean concentrations from the rainwater analyses are presented in Table 2. All samples have ionic electrical balances less than 5%, which confirm reliable analyses.

The surface water samples that were collected at the three sites along the Saloum River have average pH values from 7.8 (dry season) to 8.3 (wet season), which indicate slightly alkaline characteristics. The average surface water temperatures are close to the ambient temperature and range between 28 and 30 °C. The EC values vary along the river from 64,700 (dry season) to 50,800 μS/cm (wet season) at Foundiougne (10 km from the mouth), from 91,700 (dry season) to 60,400 μS/cm (wet season) at Lindiane (90 km from the mouth) and from 89,000 (dry season) to 55,200 μS/cm at Kaolack (120 km from the mouth). These results show that the salinity of the Saloum River substantially exceeds seawater salinity values and support the inverse estuary character of the Saloum River with gradually upstream increase of salinity. However, the decrease observed at Kaolack is probably due to the inflow of fresh groundwater as shown in the piezometric map (Fig. 4).

Temperatures of the groundwater samples range from 27.7 to 30.9 °C and from 26.4 to 33 °C in the dry and wet seasons, respectively. The pH values vary between 3.7 and 7 during the dry season and between 4.6 and 8.8 during the wet season. The lowest acidic values (pH 3–5) are found in well S49, which is located near the mangrove area, and could be due to the oxidation of pyrite, which is characteristic of mangrove degradation groundwater conditions (Ford et al., 1992). The measured EC values range from 74 to 3430 μS/cm and from 47 to 2040 μS/cm in the dry and wet seasons, respectively. According to World Health Organisation WHO (2008), this broad range of EC values differentiates two types of groundwater in the system:

1-fresh water with EC values lower than 900 μS/cm. This group comprises water sampled from wells in the western and central parts of the region;

-saline and/or polluted waters with EC values higher than 900 μS/cm. These samples originate from the coastal areas, near the Saloum River and from a few wells in the central part of the study area.

4.2. Groundwater quality assessment

The evaluation of the chemical characteristics of the groundwater samples using the descriptive statistic approach shows an order of relative abundance (in meq/L) of $Ca^{2+} > Na^+ > Mg^{2+} > K^+$ and of $HCO_3^- > Cl^- > NO_3^- > SO_4^{2-}$. It is the case for both campaigns (dry and rainy season). A high variability between the minimum and maximum values (Fig. 7) is observed. The concentrations of SO_4^{2-} and NO_3^-, and to a lesser extent Ca^{2+}, Mg^{2+} and HCO_3^-, are higher for the groundwater sampled during the rainy season. This was probably the result of the infiltration of polluted water and the dissolution of calcite and dolomite during infiltration. The concentrations of Na^+ and Cl^- in these groundwater samples decrease less, which is probably due to dilution by recharge water. Most of the major ion concentrations are within the WHO ranges for drinking water except for some cases in which the highest values of sodium Na^+, Cl^-, NO_3^- and SO_4^{2-} exceed the drinking water threshold. This suggests saline water intrusion and anthropogenic contamination as shown by the EC values. The shallowest wells (S23, S49 and S52) are characterized by high NO_3- contents (195, 200 and 327 mg/L, respectively) due to local contamination from domestic waste and pastoral activities around the wells. The highest SO_4^{2-} concentration of 582 mg/L is recorded in well S49 and is associated with high concentrations of Cl^- (215 mg/L), Na^+ (111 mg/L), Ca^{2+} (214 mg/L), Mg^{2+} (53 mg/L), K^+ (46 mg/L) and NO_3^- (200 mg/L). This well is located at Nema village close to the mangrove ecosystem probably reflects the impact of saline water intrusion and associated processes (gypsum dissolution and/or pyrite oxydation) and anthropogenic pollution at well head.

4.3. Groundwater classification using the SOMs method

The SOMs method applied to both datasets (rainy and dry seasons) exhibits similar pattern and in this paper we only describe results obtained from the dry season in Fig. 8a and b. The component maps of Cl^-, Na^+, Ca^{2+} and Mg^{2+} (Fig. 8a) show similar distribution patterns to EC map, which indicates that these ions are highly correlated with EC and that dilution is the main factor inducing variability. The high correlation between Na^+ and Cl^- suggests a common origin from the dissolution of halite and/or saltwater intrusion. To a lesser degree, HCO_3^- correlates to Ca^{2+}. The pH and HCO_3^- also have similar maps but, as is commonly found in groundwater, are inversely correlated with the CO_2 pressure.

Table 1
Physico-chemical measurements and results for groundwater samples and Saloum River samples (FL1, FL2 and FL3), for dry and rainy (wet) seasons campaigns, and groundwater isotopic data for the wet season.

Parameters	EC		T		pH		Ca^{2+}		Mg^{2+}		Na^{+}		K^{+}		HCO_3^{-}		Cl^{-}		SO_4^{2-}		NO_3^{-}		$\delta^{18}O$	$\delta^{2}H$
Units	(µS/cm)		°C			mg/l																‰		
ID	Dry	Wet	Dry	Wet	Dry	Wet	Dry	Wet	Dry	Wet	Dry	Wet	Dry	Wet	Dry	Wet	Dry	Wet	Dry	Wet	Dry	Wet	Wet	
S1	688	**551**	30.3	29.9	5	7.4	22.4	30	8.5	8.8	58.9	55.6	3.6	3.4	9.8	19.5	120.1	106.1	0.9	1.9	59.2	67.3	−4.5	−32.5
S2	612	360	30	29	5.6	6.8	43.9	37	4.9	4.4	38.9	19.3	5.8	2.9	65.9	25.6	76.4	58.5	8.3	1.8	65.5	51.4		
S3	493	453	29.5	30.2	6.7	7.4	58.3	70	2.6	3.4	11.5	10.6	1.9	3.2	177.6	188.8	25	26.7	2.6	3.4	1.7	18.5		
S4	369	289	29	30.8	6.2	7	39.1	41	2.9	2.9	15	15.7	0.7	0.5	131.4	126.8	23.5	22.8	1.4	1.3	5.9	5.2		
S5	388	317	29.4	30.8	6.6	7.6	44	50.3	1.7	1.6	12.9	13.9	2.6	2	149.8	155.6	15.9	17	3.7	3.7	2.2	4.8		
S6	185	225	29	29.2	6	7.9	17.8	30.3	1	1.7	12.9	13.7	1.1	2	58.5	106	8.6	9.4	1.1	1.8	9.8	6.7		
S17	191	**231**	28	29.8	5.5	7.2	16.5	27	1.1	1.6	13.7	16.7	0.5	1	36.6	59.7	11.1	14.3	0.2	0.6	28.2	43.9	−5.1	−35.2
S18	570	500	30	31.1	6.6	7.5	81.3	86.3	5	5.3	14.2	14.3	1.8	1.9	300.2	298	9.4	11.9	0	0.6	0	3.4	−5.2	−35.9
S19	341	313	30	30.6	6.5	7.6	50.6	59.4	0.9	0.8	5.3	5.9	4.1	3.7	163	183.2	5.7	7.6	1.3	1.4	0.8	2.2		
S20	900	748	29	30.1	7	8.1	116.4	109	9.1	9.3	32.9	30.7	1.1	1	332.9	314.9	79.8	72.2	3.5	3.8	0	3.8	−5.1	−34.7
S21	268	194	29.1	29.7	6.5	7.4	34.3	30.7	1.4	1.8	8.1	7.7	0.9	0.9	101	81.2	8.6	8.1	1.4	0.9	14.1	22.3		
S22	980	781	29	29.6	5.5	5.9	51.2	52.1	6.2	7.4	81.1	83.8	1.4	1.3	65.9	64.7	185.4	180.4	10.6	11.4	5	7	−5.1	−35
S23	1040	**890**	29	29.2	6.2	7.5	109.1	106	11.1	12.1	39.6	40.4	7.9	8.4	162	130.4	86.7	94	3.5	3	176	196		
S24	669	575	29.5	29.2	6.5	7.7	72.4	75.2	7.1	6.7	32.7	33.3	1.4	2	227.5	219	58.9	64.5	3.8	5.4	9.4	9.3		
S25	296	231	29	33	5.4	7.4	12.6	13.3	1.9	1.8	26.1	25.8	0.5	0.4	17.1	22	25.9	23.6	0.5	0.7	57.5	57.8		
S26	391	333	29.2	30.4	6	7.5	39.6	44.8	8.1	8.9	9.8	10.5	3.5	3.8	152.4	156	15.5	19.3	2.1	2.2	9.7	13.5	−5.1	−34.9
S27	294	224	29	31	5.9	7.9	19.3	18.8	2.8	2.8	20.7	20.1	0.5	0.5	46.3	46.3	30.9	31.5	0.9	0.7	22.9	23.2		
S28	1160	908	29.2	30.1	7	7.4	113.3	102	17.2	15.2	41.9	39.3	9.3	11.3	194	169.3	191	178.1	0	2.7	0	4.5		
S29	490	**492**	29.8	30.1	6.4	7.3	59.2	71.7	6.1	6.1	13.7	18.8	1.9	5	181.4	222.2	23.5	34.5	2.3	1.8	18.8	10.1		
S30	138	98	29.2	31.1	5.5	8	8.4	8.3	3.2	3.4	6.3	6.3	0.5	0.6	26.9	29.3	7.1	8	9.6	10.8	1	1.1	−5.2	−35.5
S32	125	101	29	28.9	5.3	7.8	5.1	5.1	1.1	1.1	14.1	13.3	0.8	1.1	15.9	14.7	6.6	6.3	0.9	0.9	25.3	28	−5.2	−36.7

Parameters	EC		T		pH		Ca2+		Mg^{2+}		Na^{+}		K^{+}		HCO_3^{-}		Cl^{-}		SO_4^{2-}		NO_3^{-}		$\delta^{18}O$	$\delta^{2}H$
Units	(µS/cm)		°C			mg/l																‰		
ID	Dry	Wet	Dry	Wet	Dry	Wet	Dry	Wet	Dry	Wet	Dry	Wet	Dry	Wet	Dry	Wet	Dry	Wet	Dry	Wet	Dry	Wet	Wet	
S33	362	308	30.2	30.3	6	7.6	39	43.5	4	4.3	14	14.9	0.8	0.6	104.8	104.8	23.8	26	1.1	1.5	24.6	29		
S34	950	1525	30.1	28.7	6.1	8	48.8	124.4	6.8	22.4	89.4	113.2	12	33.5	63.3	91.1	134.2	221.8	5.4	19.8	108.5	314	−4.5	−32.1

Table 1 (*Continued*)

Parameters	EC		T		pH		Ca2+		Mg^{2+}		Na^{+}		K^{+}		HCO_3^{-}		Cl^{-}		SO_4^{2-}		NO_3^{-}		$\delta^{18}O$	$\delta^{2}H$
S35	827	995	28	28.7	5.8	8.4	28.4	38.5	7.5	11.2	97.3	130.1	4.1	6.6	24.4	22	184	250.3	10	10.9	24.5	32.2	−4.1	−31.2
S36	480	550	29	29	5.8	6.9	31.3	41.5	3.8	5.7	39	55.6	0.7	1.6	39	89	47.2	78.3	4.9	13.2	78.7	54.5	−4.1	−31.7
S37	419	197	29.2	30.6	4.1	8.8	19	25.3	6.1	2.6	27.7	10.6	2.4	2.4	1.9	42.6	62.1	23.9	0	1.2	66.3	24	−4.2	−31.3
S38	730	760	29	30.1	6.1	8	58	74.8	4.7	6	58.4	62.8	0.9	1	87.7	126.7	116.3	139.9	1.6	3.1	39.2	40.1		
S39	253	217	30	29.4	5.7	8.6	15	17.9	1.9	2	20.8	22.6	0.5	0.4	48.8	50	23.9	23.3	0.6	0.9	25.2	30.8		
S40	184	175	30.5	33.5	4.9	8.4	6.9	10	1.9	2.4	11.9	14.5	6.1	7.4	7.4	11	26	29.1	0.5	1	24.1	28.3		
S41	280	286	29.4	29	4.7	8	9.3	18.1	1.5	2.7	23.7	29.4	0.3	0.4	3.9	12.3	31.6	36.5	0.3	1	49.5	68.4	−5	−33.9
S42	528	1583	27.7	26.4	5.2	8.1	28	124.4	6.3	22.5	33.8	138.5	5.6	6.5	13.5	60.9	108.2	390.2	2.3	8.8	12.7	90.3	−4.5	−31.1
S43	216	278	28.7	30	5.4	8.6	11.6	20.2	1.2	2.4	17.3	29.5	0.3	0.3	22	22	23.6	46.3	0.3	1	27.8	48.7		
S44	355	332	29.8	29.4	4.9	7.4	14.7	18.5	3	3.9	28.3	34.5	0.9	1.1	14.8	13.5	32	39.1	0	0.6	71.9	86.2		
S45	185	147	29.3	29.3	5.7	7.9	12.4	11.4	0.7	0.7	16	15.3	0.5	0.6	36.6	36.6	13.6	13.4	0.7	0.6	17.3	18		
S46	342	286	30.1	29.8	4.4	7.2	6.1	7	2.8	3.3	35	37.5	1.4	1.4	5.2	3.8	30.2	34	0	0.6	72.8	80.8		
S47	74	58	30.9	31.1	5.2	7.6	1.5	6	0.2	0.3	6.2	4.4	0.6	0.5	12.3	14.7	2.9	3.6	0.6	0.6	7.9	15.1	−5.1	−33.7
S48	3430	239	27.7	28.8	6.7	7.9	260.4	30.9	38.3	0.4	324.3	13.8	3.7	0.1	323.4	34.1	870	47.4	34	3.5	0	0.5		
S49	2191	2040	28.9	27.9	3.7	4.6	124.8	213.7	37.5	52.9	91.9	110.6	58.8	45.8	16.3	7.6	173.5	214.9	426.8	583	203.8	200	−4.7	−32.1
S50	111	125	29.6	29.8	5.4	7.5	6.7	14.6	0.5	0.6	7.9	9	0.2	0.1	20.8	48.8	11.5	11.5	0.9	1.1	0.9	0.2	−5.4	−34.9
S51	81	47	30	28.3	5.3	7.8	3.2	2.1	0.2	0.4	6.8	7.3	0.2	0.2	13.5	9.8	2.6	2.8	0.2	0.1	12.1	12.3	−5.2	−34.2
S52	1140	995	28.2	28.7	3.8	5.9	49.2	53.8	14.1	16.6	98.1	90	2.3	4	13.6	6.5	110.1	104.9	1.2	1.6	296.7	328		
S53	176	98	29.5	29.3	5.1	7.8	7.2	9.8	1.1	0.9	9.2	8	0.9	0.7	22	24.4	9.2	7.2	1	0.9	12.1	15.7		

Parameters	EC		T		pH		Ca^{2+}		Mg^{2+}		Na^{+}		K^{+}		HCO3		Cl^{-}		SO_4^{2-}		NO_3^{-}		$\delta^{18}O$	$\delta^{2}H$
Units	(μS/cm)		°C				mg/l															‰		
ID	Dry	Wet	Dry	Wet	Dry	Wet	Dry	Wet	Dry	Wet	Dry	Wet	Dry	Wet	Dry	Wet	Dry	Wet	Dry	Wet	Dry	Wet	Wet	
S62	407	388	29.6	29.6	5.2	6.1	23.3	31.9	5.5	6.8	25.2	26.5	3.6	3.6	25.6	40.2	32.8	34	0.8	1	86	93.3		
S64	75	54	29.1	31.3	4.8	6.2	5.8	5.7	0.8	0.8	4	3.9	0.2	0.2	28.2	27	3.6	3.5	0.1	0.1	0.4	0.4	−5.4	−36
Min	75	47	27.7	26.4	3.7	4.6	**1.5**	**2.1**	**0.2**	**0.3**	**4**	**3.9**	**0.2**	**0.1**	**1.9**	**3.8**	**2.6**	**2.8**	**0**	0.1	0	0.2	−5.4	−36.7
Max	3430	2040	30.9	33	7	8.8	260.4	213.7	38.3	52.9	324.3	138.5	58.8	45.8	332.9	314.9	870	390.2	426.8	583	296.7	328	−4.1	−31.1
Avg	554.18	465.8	29.3	29.8	5.63	7.49	41.49	45.73	5.7795	6.339	36.28	33.6	3.609	3.998	81.03	80.29	70.19	63.11	12.54	16.3	40.35	49.8	−4.1	−31.1
FL1	64700	50800	27	28.9	7.8	8.1	690.7	424.7	2010.7	1226	17455	10389	718.6	383.7	174.8	142.8	29641	16918	4155	2435	0	0	−0.1	−5.4
FL2	91700	60400	30	31.3	7.8	8.3	956	570.1	3679.3	1510	30053	12707	1086	399.8	206.4	151.1	52933	20857	7458	2984	0	0	0.3	−5.3
FL3	89000	55200	28	29.5	7.7	8.4	1162	574.2	4036.6	1241	32652	11443	1195	481.9	215.8	147.1	60183	18518	8540	2840	0	0	0.3	−3.2

Table 2
Physico-chemical measurements and results for seawater sample (sw) and mean values of concentrations from rainwater ((K, N, F, D, S, T and W) analyses.

Parameters	CE	pH	Ca^{2+}	Mg^{2+}	Na^{+}	K^{+}	HCO_3^-	Cl^-	SO_4^{2-}	NO_3^-
Units	(µS/cm)	(/)	mg/l							
SW	39250	7.7	338.3	952	7998.9	356.2	149.1	13014	1911.7	0
K	105	6.6	3.5	0.4	2.7	1	19	6.7	2.3	5.1
N	44	6.7	2.7	0.4	0.7	0.2	14	2.3	2.8	3.1
F	17	5.2	0.7	0.1	0.7	0.3	2.2	1.7	2.3	0.8
D	27.2	5.3	1.1	0.2	0.6	1.1	2.9	1.6	4.9	1.2
S	39.8	5	2.3	0.3	0.8	5	3.7	1.5	5.9	2.7
T	24.6	6.2	2.6	0.1	0.4	0.3	8.2	1.3	2.2	1.2
W	34.4	6.7	0.7	0.2	0.5	1.8	19	1	0.7	0.9

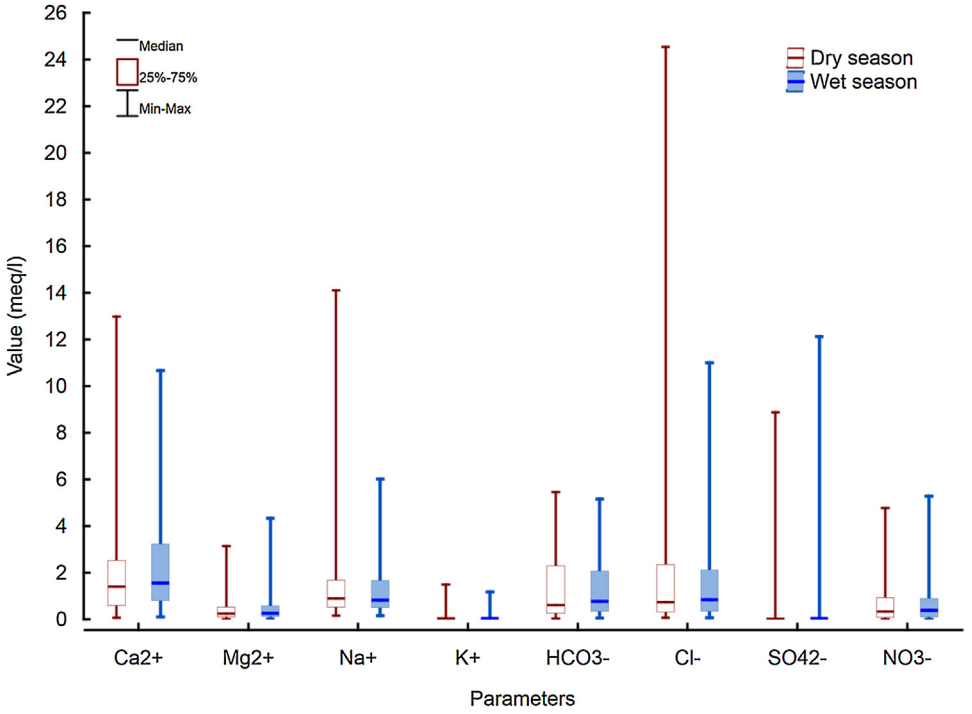

Fig. 7. Boxplot of major ions composition in CT groundwater and comparison between dry and wet seasons of 2012.

Three distinct groups were obtained with the SOMs method, which correspond to different groundwater types with respect to the contribution of each chemical parameter (Fig. 8b). The physico-chemical and chemical characteristics of these 3 groups were evaluated using a descriptive statistic approach in which the minimum, maximum, and average median of the EC and major ions were computed for each campaign (Table 2). In addition to the statistical approach, a Piper trilinear diagram (Piper, 1944) that describes the water types (Fig. 9), bivariate diagrams (Fig. 11a and b) and computed Saturation Index (SI) values (Fig. 11c) were used to further infer the various processes that control the chemical compositions of the groundwater groups.

The U-matrix (Fig. 8b), Piper diagram (Fig. 9) and Table 3 show that:

a) Group 1, which is represented by samples S1, S2, S22, S23, S34, S35, S36, S37, S38, S42, S49, S52 and S62, is characterized by high values of EC, Cl^-, Na^+, NO_3^- and SO_4^- and relatively low values of HCO_3^-. It is generally encountered near the Saloum River and in one sample near the Nema River (Fig. 10). The EC values range from 491 to 2191 during the dry season with an average of 872 µS/cm. The water types (Fig. 9) are dominantly Na–Cl (42%) and Ca–Cl (42%), and two samples (S23 and S49) exhibiting Ca–HCO_3 (8%) and Ca/Na–SO4 (8%) facies, respectively. This group includes saline water (S22, S28, S35 and S42) that is characterized by high Cl^- contents (often above 150 mg/L) as well as polluted water (S23, S34, S49 and S52) with high NO_3^- contents (above 100 mg/L). It indicates contamination of the groundwater and recent infiltration (Currell et al., 2010). Saline groundwater, seawater and the Saloum River have typical common characteristics of Na-Cl type water (Fig. 9) and molar ratios close to seawater value (0.86) (Fig. 11a).This fact confirms the marine origin of the ions (Jones et al., 1999; Vengosh et al., 1999; Faye et al., 2001, 2003, 2004; Vengosh, 2013). However, some samples exhibiting a relative deficiency in Na^+ relative to Cl probably reflect reverse ion exchange reaction. In this case Na^+ is taken up by the clay exchanger and Ca^{2+} is released to the solution. Magaritz and Luzier (1985) stated that groundwater samples containing less than 15% seawater are

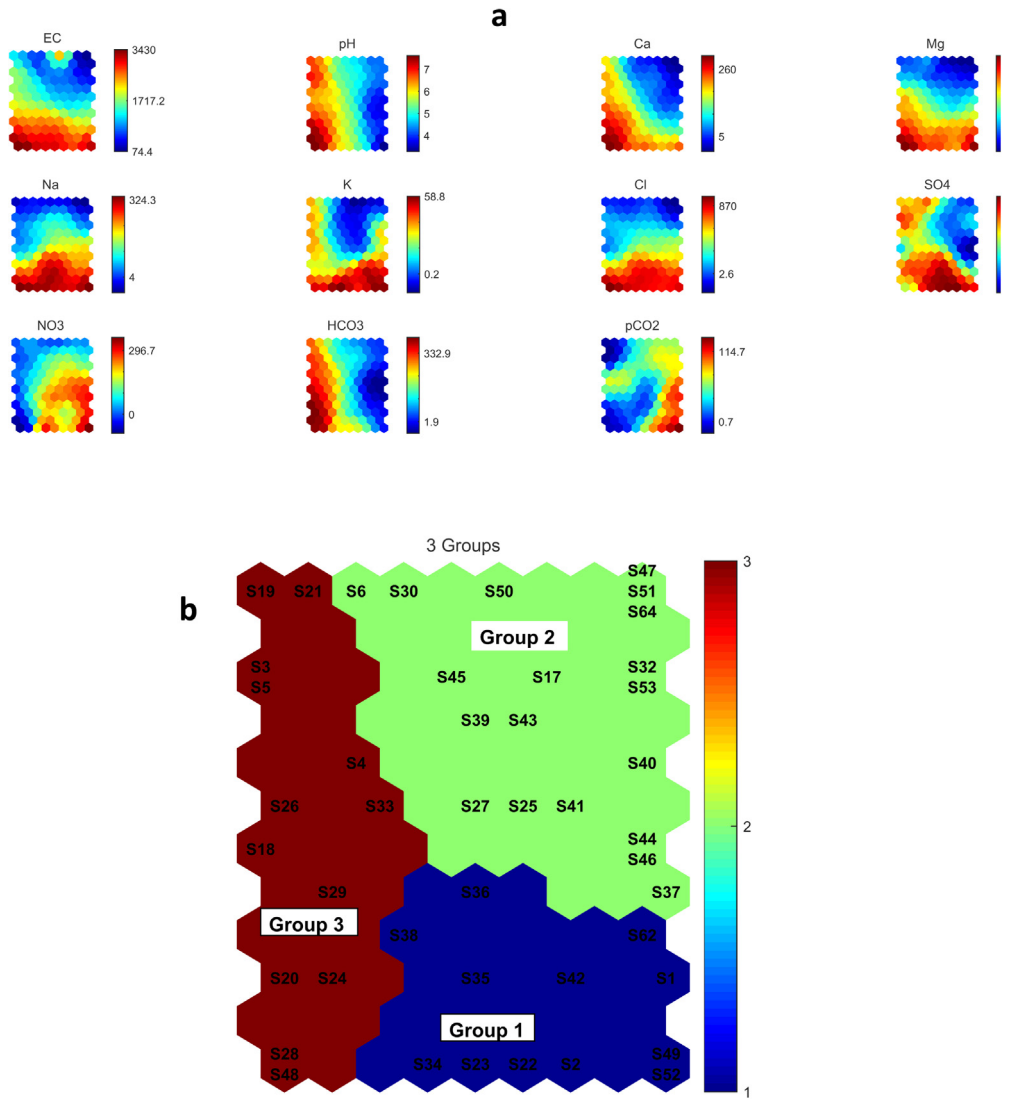

Fig. 8. a) SOMs individual components maps of the chemical parameters in the CT aquifer during the 2012 dry season and b) SOMs U-matrix and clustering in 3 groups.

enriched in Na+, and as the percentage of seawater increases. In fact, the water becomes increasingly enriched in Ca^{2+} and Na^{+} is depleted. This process leads to groundwater facies evolving from Na-Cl to Ca-Cl (Mercado, 1985; Appelo and Postma, 2005). In addition, the sampled points are aligned along a slope of −1 in the (Ca + Mg)–(SO_4–HCO_3) *versus* (Na + K)-(Cl-NO_3) diagram (Fig. 11b). This diagram excludes halite, calcite and dolomite dissolution (Jankowski and Acworth, 1997; Garcia et al., 2001; Abid et al., 2011) and evidenced ion exchange reaction as a dominant geochemical process. .

The correlation between Ca^{2+} and $SO4^{2-}$ (Fig. 8a) and the SI value (-0.97) with respect to gypsum (Fig. 11c) in the highly mineralized waters from well S49 (of Ca-SO_4 water type) show a dissolution of gypsum. This is observed in mangrove soil, and would release Ca^{2+} and $SO_4{}^{2-}$ into the groundwater (Eq. (1)). Otherwise, considering the low pH (3–5), the enrichment of $SO_4{}^{2-}$ may also result from pyrite oxidation (Eq. (2)), usually occuring in mangrove degradation soils (Lebigre and Marius, 1984; Kristensen et al., 1991)

$$CaSO_4 \Leftrightarrow Ca^{2+} + SO_4^{2-} \tag{1}$$

$$F_eS_2 + \frac{7}{2}O_2 + H_2O \Rightarrow CO_2 + \Leftrightarrow CH_2CO_3 \Leftrightarrow F_e^{2+} + 2S0_4^{2-} + 2H^{+} \tag{2}$$

b) Group 2 is represented by well samples S3, S4, S5, S18, S19, S20, S21, S24, S26, S28, S29 and S33, located in the eastern part of the region, and by sample S48 (Fig. 10), located in the coastal strip. Sample S48 characteristics differ from other samples in group 2 in that it exhibits high values of Cl^{-} (870 mg/L) and Na^{+} (324.3 mg/L) and is a Na-Cl facies. Its EC values vary seasonally (3430 and 239 μS/cm during the dry and rainy seasons, respectively). It is suggesting that this well taps the

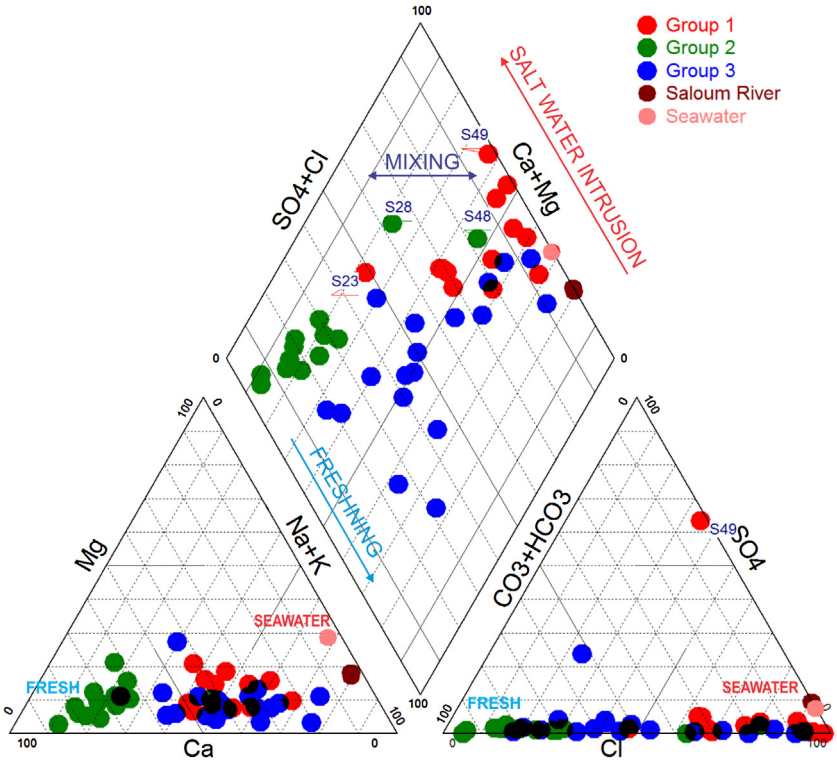

Fig. 9. Piper's diagram showing the relative chemical compositions of groundwater, Saloum River water and seawater samples collected during the 2012 dry season. Groundwater samples belonging to the three groups defined with the SOMs method are plotted with different colors.

Table 3
Summary of statistical hydrochemical data of field campaigns corresponding to dry and wet seasons for groundwater groups obtained with the SOMs analysis.

Parameters			CE	T	pH	Ca^{2+}	Mg^{2}	Na^{+}	K^{+}	HCO_3^{-}	Cl^{-}	SO_4^{2-}	NO_3^{-}
	μS/cm)	°C		mg/l									
Dry	1	min	419	28.2	3.7	19	3	25	0.6	1.9	32.7	0.8	5
		max	2191	30.3	6.2	124	14	98.1	58.7	161.9	187.3	426	296.7
		median	730	29	5.5	43.9	6.3	58.4	3.6	25.6	110.1	3.5	66.3
		average	872	29.1	5.5	50.8	9.7	62.1	8.6	48.0	110.7	39.5	100.7
	2	min	268	27.7	6.2	39.1	0.9	5.2	0.7	100	5.7	0.1	0.1
		max	1160	30	7	116.4	17	41	9.3	332.9	191	3.8	24
		median	490	29.5	6.5	54.5	4.5	13.9	1.8	170.3	23.5	1.8	4
		average	533.4	29.5	6.5	62.3	5.5	17.7	2.5	184.7	40	1.9	7.8
	3	min	74.4	28	4.4	3.2	0.2	3.9	0.1	3.8	2.9	0.1	0.3
		max	342	30.9	5.9	19.3	3.2	34.9	6.1	58.5	31.6	9.5	72
		median	185	29.5	5.35	8.8	1.2	13.9	0.5	21.4	12.5	0.5	23.5
		average	197	29.5	5.3	10	1.5	15.6	0.9	24.3	16.7	1.0	25.9
wet	1	min	388	26.4	4.6	31.9	4.3	28.5	9	6.5	33.9	1.5	6.9
		max	2040	30	8.4	213.7	52.8	138.5	45.8	169.2	390.1	582.1	314
		median	890	29	7.4	53.8	11.2	62.8	4	60.8	139.9	3.131	67.3
		average	948.2	29.0	7	79.3	14.8	74.3	10.0	65.7	157.8	50.9	113.7
	2	min	194	29.2	7	43.5	0.7	7.6	0.6	81.1	8.1	0.5	3.1
		max	748	30.8	8.1	108.7	9.2	30.7	5	314.9	72.2	5.3	29
		median	325	30.1	7.6	54.9	3.8	14.1	2.0	169.6	21.1	1.8	8.0
		average	395.6	30.2	7.6	59.3	4.4	15.8	2.2	179.7	26.7	2.3	10.7
	3	min	47	28.3	6.2	5	0.3	3.8	0.05	9.7	3.5	0.6	3.4
		max	332	31.1	8.8	30.8	3.3	35.5	7.3	59.7	46.2	5.3	22.3
		median	197	30.2	7.8	13.3	1.8	14.5	0.5	24.4	23.3	0.9	24.0
		average	180.2	30.2	7.8	14.2	1.8	17.0	1.0	27.5	21.3	1.4	30.7

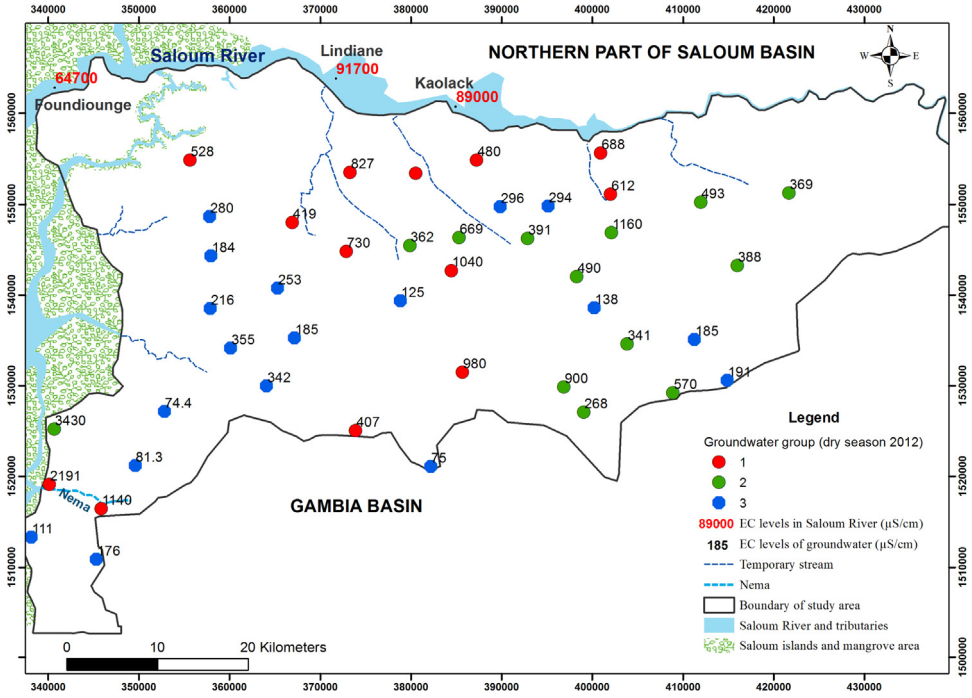

Fig. 10. Spatial distribution, during the 2012 dry season, of the three groundwater groups as obtained with the SOMs analysis.

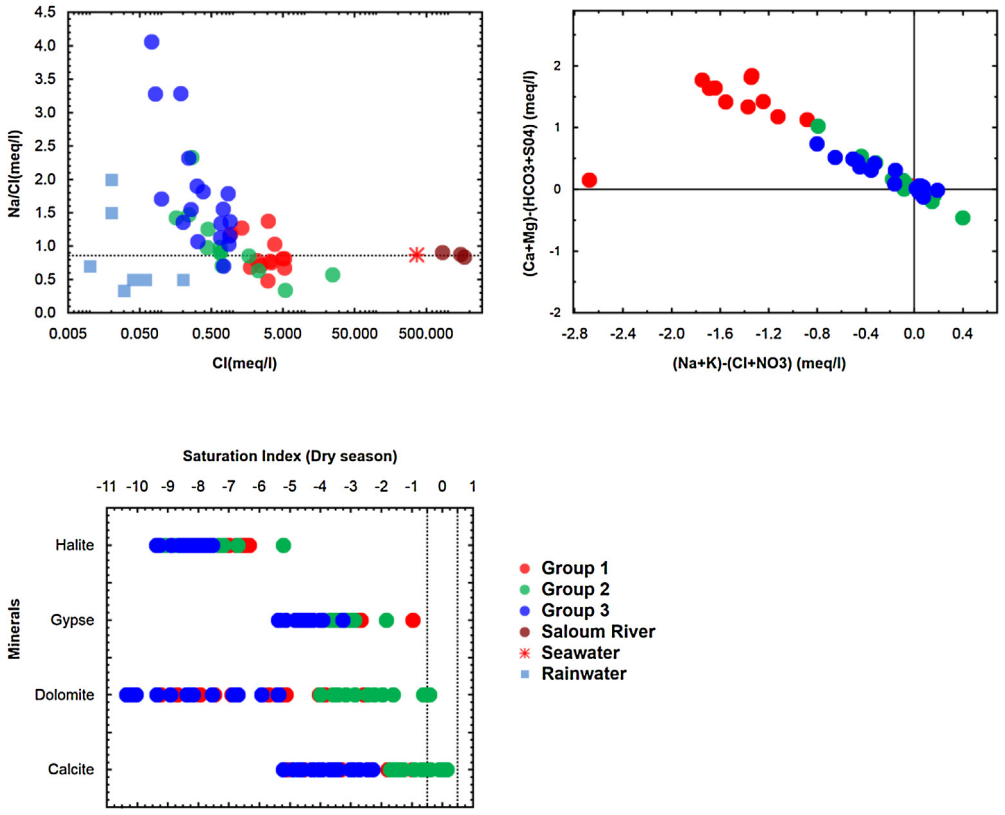

Fig. 11. Relationship between the contents of a) Na/Cl *vs* Cl, b) [(Ca+Mg)-(SO4+HCO3)] *vs* [(Na+Cl)-(Cl+NO3)] and c) saturation index value in the groundwater samples collected during the 2012 dry season. The three distinct groups are those defined with the SOMs method.

Table 4
Summary of statistical hydrochemical data of field campaigns during the wet seasons of 2003 and 2012 for groundwater groups obtained with the SOMs analysis.

Parameters			CE	Ca^{2+}	Mg^{2}	Na^{+}	K^{+}	HCO_3^{-}	Cl^{-}	SO_4^{2-}	NO_3^{-}
	μS/cm)	mg/l									
2003	1	Mean	2099.4	133.7	37.9	278.6	16.5	82.4	513.4	64.8	131.6
		Median	1769.0	140.4	29.5	202.6	8.8	61.0	386.3	12.6	59.6
		Min	1013.0	98.1	6.5	114.5	1.9	30.5	174.0	0.5	2.0
		Max	4920.0	189.8	106.2	791.7	61.8	158.6	1498.0	368.0	259
	2	Mean	486.0	41.8	4.0	48.6	1.3	134.2	88.9	4.0	10.0
		Median	358.0	46.1	3.5	21.4	1.2	134.2	23.1	0.9	7.8
		Min	35.0	5.3	0.2	2.9	0.6	39.6	1.5	0.2	1.6
		Max	1686.0	50.0	6.2	234.0	2.6	225.7	75.3	23.6	29.2
	3	Mean	216.0	16.8	3.7	20.2	2.6	58.0	20.5	1.0	49.0
		Median	172.5	11.6	1.9	14.7	0.8	47.3	19.6	0.3	26.7
		Min	62.0	3.8	0.2	6.8	0.1	27.4	2.6	0.1	5.9
		Max	299.0	56.5	17.6	37.1	19.3	131.1	30.8	5.0	199.6
2012	1	Mean	1250.6	96.0	20.7	90.3	19.8	46.2	194.4	132	124.9
		Median	1260.0	99.6	16.8	101.3	6.5	23.8	194.2	9.9	78.8
		Min	360.0	30.0	4.3	19.3	0.9	7.6	58.4	1.7	32.1
		Max	2191.0	213.0	52.8	138.5	45.8	91.1	390.0	582.4	200.1
	2	Mean	365.0	54.1	3.1	15.1	2.2	150.7	30.2	2.5	9.7
		Median	313.0	59.4	2.9	13.8	2	183.2	26.7	1.8	9.3
		Min	194.0	30.7	0.3	5.9	0.6	34.1	64.5	0.8	0.5
		Max	575.0	71.7	6.7	33.3	5.0	222.1	8.1	5.0	22.3
	3	Mean	170.5	11.6	1.8	17.3	1.3	27.1	19.6	0.7	29.6
		Median	161.0	10.7	1.4	14.9	0.6	25.7	18.3	0.7	20.6
		Min	47.0	5.0	0.3	3.8	0.1	9.7	3.5	0.9	3.4
		Max	286.0	18.7	3.9	37.5	7.3	49.9	34.0	1.0	86.8

dynamic seawater interface characterized by seawater advance during dry season followed seaward interface retreat during rainy season (i.e. when groundwater heads are higher). At the exception of S48, this group is characterized by high Ca^{2+} and HCO_3^{-} contents, relatively low Cl^{-} and Na^{+} contents and variable mineralization ranging from 268 to 1160 μS/cm with an average of 533 μS/cm during the dry season.This group is featured by fresh and uncontaminated groundwater that is nearly free of marine water contamination, and the groundwater facies are dominantly Ca–HCO_3. Computed SI values with respect to calcite (ranging between −1.7 and 0.7) and dolomite (ranging between −4 and 0.6) (Fig. 11c), and Ca/HCO_3 molar ratios (1) in addition to occurrence of calcite mineral in the reservoir matrix (as evidenced by Lappartient, 1985) reflect carbonate minerals dissolution. This reaction is the main geochemical process which would be concomitant to ion exchange in which Ca^{2+} replaces Na^{+} in the clay matrix (Fig. 11a).

c) Group 3, which is represented by well samples S6, S17, S25, S27, S30, S32, S39, S40, S41, S43, S44, S45, S46, S47, S50, S51, S53, and S64, is characterized by low mineralized groundwater. The EC values are ranged from 74.4 to 342 μS/cm in the dry season. More than 70% of the samples exhibit low EC values (below 250 μS/cm) suggesting a lower mineralisation and their water types are dominantly Na–HCO_3 (33%), Na–Cl (33%), Ca–HCO_3 (22%) and Ca–Cl (12%). These characteristics of low mineralisation and various water types likely depict the recently infiltration rainwaters. They are reaching the aquifer accompanied by both rapid cation (Na for Ca) and anion (Cl for HCO3) exchanges in the clay matrix of the aquifer reservoir in addition to calcite dissolution. This would result in a consistent groundwater-type gradation of low mineralised Ca-Cl and Na-HCO3 types evolving to Na-Cl, Ca-HCO3 to Ca-Cl and Na-Cl indicating changes along groundwater flowpaths in these zones (Mercado, 1985; Hidalgo et al., 1995).

4.4. Interannual variations of groundwater salinity between 2003 and 2012

The temporal trend variations of groundwater salinity were investigated using data collected in 2003 and 2012. In total, 28 chemical analyses were retrieved from November 2003 (Faye et al., 2004) and November 2012 (this work) as a comparison to depict changes related to anthropogenic and natural stress in this vulnerable system. Salinity patterns of the Saloum River water EC exhibits changes from 78,300 to 90,100 μS/cm in 2003 and from 50,800 to 60,400 μS/cm in 2012. These changes much likely derive from rainfall events which varied from 535 mm (502.9 mm effective rainfall) in 2003–847 mm (796.18 mm effective rainfall) in 2012. Compared with the long-term (1960–1990) average of 610 mm, considered as reference in Sahel, the 2003 and 2012rainfall records represent respectively a decline of 12% and an increase of 38%.

This high variation in rainfall between these 2 reference years would probably also change chemical patterns in the groundwater. SOMs analyses of the different groups revealed:

- In wells S1, S2, S27, S34, S35 and S38, which are generally located near the Saloum River and correspond to the group 1 in the SOMs analysis, the EC evolution shows a decreasing trend with values higher in 2003 (average of approximately 2099 μS/cm) than in 2012 (1250 μS/cm) (Table 4). The ionic contents changes, shown in the Piper diagram (Fig. 12), are featured by a shift of the groundwater types from Na-Cl to Ca-Cl or Ca-HCO_3. This confirms the enrichment of Ca relative

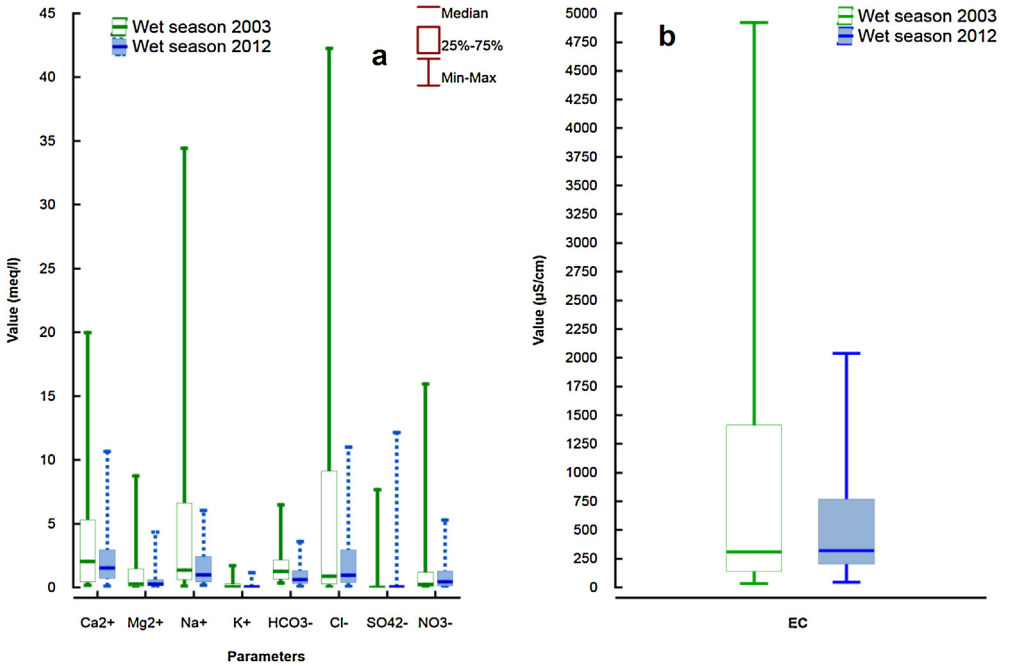

Fig. 12. Comparison of boxplot diagrams as obtained for a) major ions composition and b) electrical conductivity (EC) in CT groundwater between wet seasons of 2003 and 2012.

to Na, and therefore the softening by dilution inferred by inflows of both infiltrated rainfall and Saloum River compared to 2003 (see above).

- In wells S3, S19, S21, S22, S23, and S62, located in the central and eastern zones mostly, and corresponding to group 2 in the SOMs analysis, the EC values increased from 2003 (mean value of 353 µS/cm) to 2012 (average of approximately 587 µS/cm). This is also observed in the ionic contents of the groundwater samples as confirmed by the Piper diagram (Fig. 13). Groundwater types mostly evolved from Ca-HCO_3 to Na-Cl or Ca-Cl. These characteristics of increased mineralisation and enrichment of HCO_{3^-}, Cl^- and/or NO_3^- in some wells likely depict the recently infiltration rainwaters. It is reaching the aquifer accompanied by both combined calcite dissolution and pollutants from anthropic contamination.

- Near the coast and the Nema River, no trend can be distinguished. The EC values decreased in some of the wells (e.g., S40, S41, S48, and S50) (from 1750 to approximately 200 µS/cm) and increased in others (e.g., S42, S49, and S52) (from 974 to approximately 1539 µS/cm). In this region, the chemical evolution of the groundwater was due to a combination of seawater intrusion that was enhanced by pumping activities and dilution by recharge.

4.5. Isotope composition

Often, isotopic results greatly help for understanding the structural controls on groundwater flow in arid regions (e.g. Dailey et al., 2015) and the recharge patterns (among many others: Shahul Hameed et al., 2015). Here, the results of the isotope analyses of the surface water and groundwater samples are presented in Table 1. Isotopic analyses were only performed on a subset of samples that were collected in November 2012, which corresponds to the end of the rainy season. The $\delta^{18}O$ and $\delta^{2}H$ values of the groundwater samples and the Saloum River water are plotted against the Global Meteoric Water Line (GMWL) and the Local Meteoric Water Line (LMWL) of equation ($\delta^{2}H = 7.93\delta^{18}O + 10.09$) defined by Travi et al. (1987) (Fig. 14a).

The Saloum River samples are distinctly enriched with values ranging from −0.11 to +0.32‰ for $\delta^{18}O$ and from −5.4 to −3.2‰ for $\delta^{2}H$. These samples deviate significantly from the SMOW values (Fig. 14a) confirming prominent evaporation processes affect the low to stagnant Saloum River water. In the groundwater samples, the $\delta^{18}O$ values range from −5.4 to −4.1‰, and the $\delta^{2}H$ values range from −36 to −31‰, with mean values of −4.9‰ and −33‰, respectively. Plotted in the $\delta^{2}H$ *vs.* $\delta^{18}O$ diagram, the data cluster below the LWML along the line $\delta^{2}H = 3.9\ \delta^{18}O - 14.3$ ($R^2 = 0.83$). The samples plot to the right of the global meteoric indicates an enrichment of heavy isotopes, and suggests that they were subjected to variable degrees of evaporation

Indeed, in the Saloum environment, where temperatures (mean 28,5 °C) are high as well as evapotranspiration (2030 mm/year), it is likely that recharge water from rainfall evaporates before and/or during after infiltration.

Two distinct clusters can be distinguished in the groundwater samples using the isotopic data (Fig. 14a). In cluster A, the stable isotope values range from −5 to −4.1% for $\delta^{18}O$ and from −35 to −31% for $\delta^{2}H$. This cluster represents samples of group

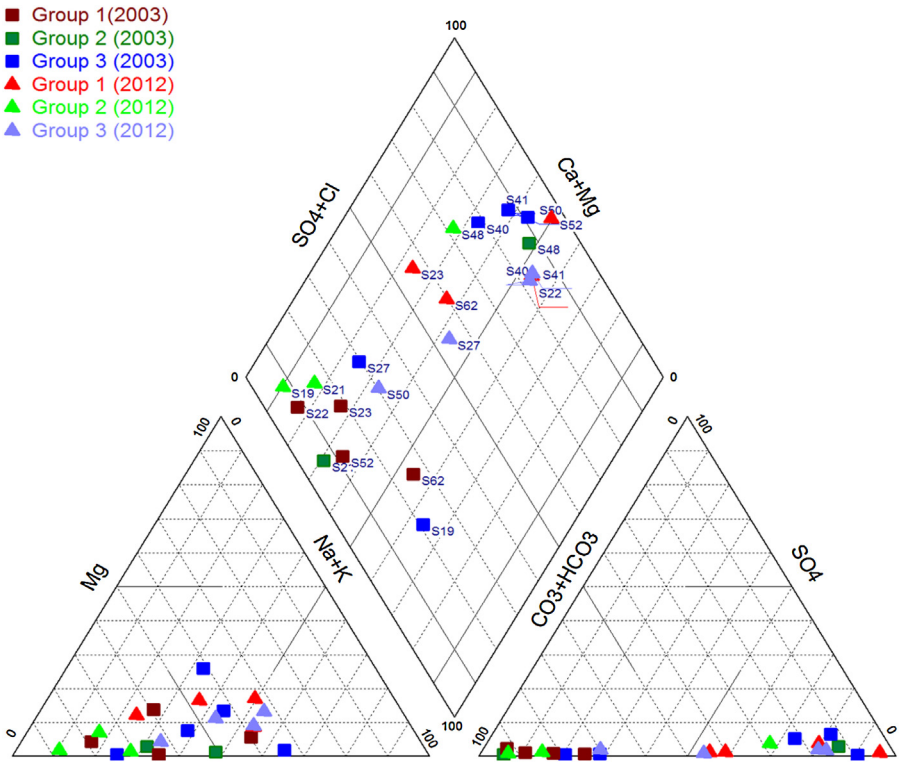

Fig. 13. Piper diagram showing groundwater composition change between wet seasons of 2003 and 2012.

1, which are located along the coast and near the Saloum River. Cluster B is characterized by more depleted stable isotope values with $\delta^{18}O$ ranging from −5.4 to −5.1% and $\delta 2H$ ranging from −36 to −34%. This cluster represents fresh groundwater samples of groups 2 and 3. The groundwater of cluster A appears to be more affected by evaporation or is more influenced by the intrusion of evaporated surface water. By comparing $\delta^{18}O$ and Cl^- (Fig. 14b), the existence of the two previous clusters is confirmed. The samples of cluster A are located on a mixing line that joins the samples of cluster B, which represent fresh water, and the samples from the Saloum River and the ocean. This confirms that the salinization of the samples of cluster A is caused by mixing with coastal marine or Saloum River waters.

The results suggested that the CT aquifer in the investigated areas have been recharged by

rainwater infiltration and mixed with saline surface water from the Saloum River, which is also affected by high evaporation processes. Faye et al. (2004) hypothesized five processes may lead to this scattered pattern: 1) mixing process along flow paths combined with evaporation from the shallow water table; both can homogenise the $\delta^{18}O$ values and increase the overall salinity; (2) the isotopic contents of recharged waters and the Saloum River water can have a wide range and also homogenization of $\delta^{18}O$ values; (3) transpiration from vegetation cover; (4) dissolution of the salt minerals may lead to changing both the Saloum River hydrochemistry as well as the interstitial water chemistry increasing therefore salinity in the transition zone; (5) to a lesser extent, the salt secreting halophytes plants of the mangrove system located at the mouth of the estuary may lead to the enrichment of salinity in the unsaturated zone without isotopic fractionation.

As shown in Fig. 14c, the Saloum River was notably depleted in heavy isotopes in November 2012 in comparison to November 2003, which values range from 1.5 to 1.7‰ for $\delta^{18}O$ and from 0 to 3‰ for $\delta^{2}H$. Otherwise, the evaporated trend of the 2003 groundwater samples deviates more significantly (slope of 3.9) from the LMWL than those of the 2012 samples (slope of 4.9) (Fig. 14c). These results suggest the dilution of the Saloum River water and the freshening of groundwater near the river due to the increasing amount of fresh water from rainfall between 2003 and 2012 (Fig. 14c).

5. Conclusions

The CT aquifer represents an important groundwater resource in Senegal and particularly in the Saloum region, where it is the main source of drinking water for the local population. Therefore, the reassessment of processes responsible for the observed mineralization and degraded water quality and of the groundwater quality changes of the CT aquifer is of great importance. This reassessment must be done in the light of the new constraints (e.g. changes in climatic conditions and pumping constraints), and the new flow pattern configuration in this system. The simultaneous analysis of hydrogeochemical and isotopic data using conventional and statistical methods allows the assessment of the groundwater quality in the

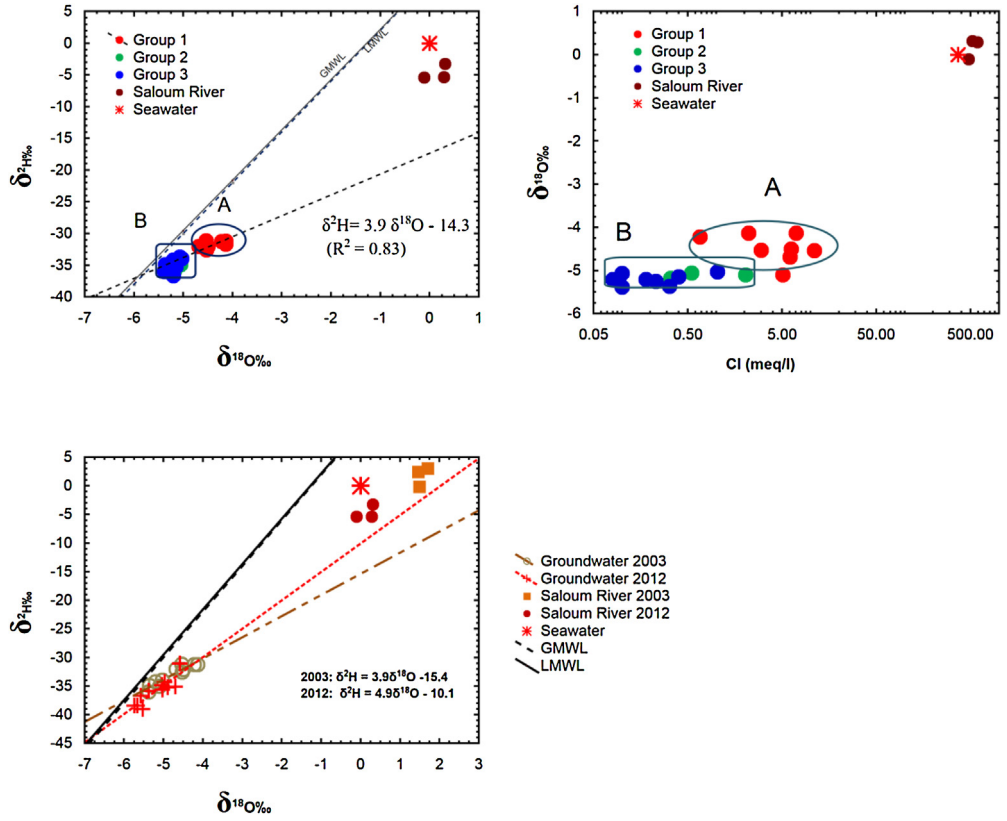

Fig. 14. Relationship between a) δ^2H and $\delta^{18}O$ and b) $\delta^{18}O$ and Cl in the CT groundwater during the 2012 wet season and c) δ^2H and $\delta^{18}O$ in the CT groundwater during the wet seasons of 2003 and 2012. The groundwater samples are classified using the three groups defined with the SOM's method.

southern part of the Saloum Basin. Statistical analyses of the geochemical data demonstrate the spatial variability of the chemical characteristics of the groundwater. They allow to distinguish three groups of groundwater. The first group (1), which is located near the coast and near the Saloum River, is affected by mixing with saline water intrusion and/or anthropogenic pollution, and the main facies are Na-Cl or Ca-Cl types. The second group (2), which is mainly located in the central and eastern parts of the study area, is less mineralized and contains Ca-HCO_3 facies as a result of calcite dissolution due to interaction with the aquifer. In the third intermediary group (3), some samples indicated freshening processes likely depicting the effect of recent infiltration rainwaters.

These three groups and their chemical characteristics are generally observed in both the dry and wet seasons. However, a decrease of the mineralization is generally observed during the wet season due to the recharge of less mineralized water.

A comparison of the groundwater quality characteristics in terms of salinization between 2003 and 2012 indicates that significant changes have occurred. In the wells that are located near the Saloum River, decreases of the Na+ and Cl- concentrations and the EC values are observed. The groundwater facies have generally evolved from Na-Cl to Ca-Cl or Ca-HCO_3, which indicates the dilution of groundwater due to freshening in the vicinity of the Saloum River. This freshening is due to an increase of rainfall as well as the intrusion of less mineralized water in recent years as the salinity of the Saloum River has also decreased. An increase of mineralization is observed in some wells located in the central and eastern zones of the study area. Groundwater types mostly evolved from Ca-HCO_3 to Na-Cl or Ca-Cl and indicate recent infiltration rainwaters reaching the aquifer accompanied by both combined calcite dissolution and pollutants from anthropic contamination. No trend can be distinguished near the coast and the Nema River where the chemical evolution of the groundwater was due to a combination of seawater intrusion and dilution by recharge.

In summary, changes of groundwater levels and quality have been observed in the CT aquifer between 2003 and 2012 in response to variations in the precipitation regime and other factors. Additional changes in recharge or in the flow regime will occur in the near future in response to climate change or to increases of groundwater pumping. It is thus important to identify the evolution of the groundwater quality that is caused by these new changes to avoid or mitigate the future degradation of groundwater quality before it becomes a major obstacle to the future economic development of this coastal area.

Acknowledgments

The authors thank the International Foundation of Sciences, Francophone University Agency and the ANGLE project for financial support to carry out this work. They also thank the Hydrogeology Laboratory of the University of Liège< (Belgium), the Department of Geology of Cheikh Anta Diop University in Dakar (Senegal) and the Helmholtz Zentrum München, Institute of Groundwater Ecology (Neuherberg/Germany). The authors are grateful to the two anonymous reviewers who helped a lot for improving the paper.

Appendix A. Supplementary data

Supplementary data associated with this article can be found, in the online version, at http://dx.doi.org/10.1016/j.ejrh.2016.12.082.

References

Abid, K., Zouari, K., Dulinski, M., Chkir, N., Abidi, B., 2011. Hydrologic and geologic factors controlling groundwater geochemistry in the Turonian aquifer (Southern Tunisia). Hydrogeol. J. 19 (2), 415–427, http://dx.doi.org/10.1007/s10040-010-0668-z.
Allen, R., Pereira, L., Raes, D., 1998. Crop Evapotranspiration – Guidelines for Computing Crop Water Requirements – FAO Irrigation and Drainage Paper 56. Food and Agriculture Organization of the United Nations (FAO).
Appelo, C.A.J., Postma, D., 2005. Geochemistry, Groundwater and Pollution, second ed. Balkema Rotterdam (656p).
Aranyossy, J.F., Guere, A., Sidoro, M., 1989. Étude par les isotopes de l'environnement des dépressions piézométriques; premières données sur des exemples au Mali. Hydrogéologie 3, 151–158.
Archambault, J., 1960. Les Eaux Souterraines d'Afrique Occidentale. Berger Levrault, Nancy, 139p.
Barusseau, J.P., Diop, E.H.S., Saos, J.L., 1985. Evidence of dynamics reversal in tropical estuaries, geomorphological and sedimentological consequences (Saloum and casamance rivers, Senegal). Sedimentology 32 (4), 543–552.
Belkhiri, L., Mouni, L., Boudoukha, A., 2012. Geochemical evolution of groundwater in an alluvial aquifer: case of El Eulma aquifer, East Algeria. J. Afr. Earth. Sci. 66–67, 46–55, http://dx.doi.org/10.1016/j.jafrearsci.2012.03.001.
Bellion, Y.J.C., 1987. Histoire géodynamique Post-paléozoïque De l'Afrique De l'Ouest d'après l'étude De Quelques Bassins sédimentaires (Sénégal, Taoudéni, Iullemmeden, Tchad). Thèse Sciences. Univ. Avignon, 296p.
Conrad, G., Lappartient, J.R., 1987. The Continental terminal; its position within the Cenozoic geodynamic evolution of the Senegalo-mauritanian basin. J. Afr. Earth Sci. 6 (1), 45–60.
Coplen, T.B., 1988. Normalization of oxygen and hydrogen isotope data. Chem. Geol. 72, 293–297.
Currell, M.J., Cartwright, I., Bradley, D.C., Han, D., 2010. Recharge history and controls on groundwater quality in the Yuncheng Basin, North China. J. Hydrol. 385, 216–229, http://dx.doi.org/10.1016/j.jhydrol.2010.02.022.
Dailey, D., Sauck, W., Sultan, M., Milewski, A., Ahmed, M., Laton, W.R., Elkadiri, R., Foster, J., Schmidt, C., Al Harbi, T., 2015. Geophysical, remote sensing, GIS, and isotopic applications for a better understanding of the structural controls on groundwater flow in the Mojave Desert, California. J. Hydrol.: Reg. Stud. 3, 211–232.
Degallier, R., 1962. Hydrogéologique du ferlo septentrional (Sénégal). Mémoire BRGM 19, 44 p.
Dieng, N.M., Faye, S., Dinis, J., Gonçalves, M., Caetano, M., 2014. Combined uses of supervised classification and Normalized Difference Vegetation Index techniques to monitor land degradation in the Saloum saline estuary system. In: Diop, S., et al. (Eds.), The Land/Ocean Interactions in the Coastal Zone of Westand Central Africa, Estuaries of the World. , 10.1007/978-3-319-06388-1_2.
Diluca, C., 1976. Hydrogeology of the Continental Terminal Aquifer Between the Sine and the Gambia. Technical Report. BRGM Dakar, 33p.
Diop, E.S., 1986. Tropical Holocene Estuaries. Comparative Study of the Physical Geography Features of the Rivers from the South of Saloum to the Mellcorée (Guinea Republic). (PhD. Thesis). Univ. Louis Pasteur, Strasbourg, France.
Edmunds, W.M., Gaye, C.B., 1994. Estimating the spatial variability of groundwater recharge in the Sahel using chloride. J. Hydrol. 156 (1–4), 47–59, http://dx.doi.org/10.1016/0022-1694(94)90070-1.
Favreau, G., Leduc, C., Marlin, C., Guéro, A., 2002. Une dépression piézométrique naturelle en hausse au Sahel (Sud-Ouest du Niger). C.R. Geosci. 334 (6), 395–401, http://dx.doi.org/10.1016/S1631-0713(02)01763-7.
Faye, S., Evans, D., Cissé Faye, S., 2001. Origin and distribution of saline groundwater in the Saloum (Senegal) coastal aquifer, proceed. In: Second International Conference on Saltwater Intrusion and Coastal Aquifers, Mérida, Yucatán, México.
Faye, S., Cissé Faye, S., Ndoye, S., Faye, A., 2003. Hydrogeochemistry of the Saloum (Senegal) superficial coastal aquifer. Environ. Geol. 44 (2), 127–136, http://dx.doi.org/10.1007/s00254-002-0749-y.
Faye, S., Maloszewski, P., Stichler, W., Trimborn, P., Cissé Faye, S., Gaye, C.B., 2004. Groundwater salinization in the Saloum (Senegal) delta aquifer: minor elements and isotopic indicators. J. Sci. Total. Environ., 17, http://dx.doi.org/10.1016/j.scitotenv.2004.10.00.
Faye, S., Diaw, M., Ndoye, S., Malou, R., Faye, A., 2009. Impacts of climate change on groundwater recharge and salinization of groundwater resources in Senegal. In Proc. Groundwater and Climate in Africa, Kampala, IAHS Publ, 334: 163–173.
Faye, S., Ba, M.S., Diaw, M., Ndoye, S., 2010. The groundwater geochemistry of the Saloum delta aquifer: importance of silicate weathering, recharge and mixing processes. J. Afr. Environ. Sci. Tech. 4 (12), 815–830, http://dx.doi.org/10.5897/AJEST09.180.
Ford, M., Tellam, J.H., Hughes, M., 1992. Pollution-related acidification in the urban aquifer, Birmingham, UK. J. Hydrol. 140 (1-4), 297–312, http://dx.doi.org/10.1016/0022-1694(92)90245-Q.
Güler, C., Thyne, G.D., McCray, J.E., Turner, A.K., 2002. Evaluation of graphical and multivariate statistical methods for classification of water chemistry data. Hydrogeol. J. 10 (4), 455–474, http://dx.doi.org/10.1007/s10040-002-0196-6.
Gamble, A., Babbar-Sebens, M., 2012. On the use of multivariate statistical methods for combining in-stream monitoring data and spatial analysis to characterize water quality conditions in the White River Basin, Indiana. USA. Environ. Monit. Assess. 184 (2), 845–875, http://dx.doi.org/10.1007/s10661-011-2005-y.
Garcia, L.A., Shigidi, A., 2006. Using neural networks for parameter estimation in groundwater. J. Hydrol. 318 (1–4), 215–231, http://dx.doi.org/10.1016/j.jhydrol.2005.05.028.
Garcia, M.G., Hidalgo, M., Blessa, M.A., 2001. Geochemistry of groundwater in the alluvial plain of Tucuman province. Argentina Hydrogeol. J. 9 (6), 597–610, http://dx.doi.org/10.1007/s10040-001-0166-4.
Ghesquière, O., Walter, J., Chesnaux, R., Rouleau, A., 2015. Scenarios of groundwater chemical evolution in a region of the Canadian Shield based on multivariate statistical analysis. J. Hydrol.: Reg. Stud. 4(B, 246–266.
Gning, A.A., 2015. Etude Et Modélisation Hydrogéologique Des Interactions Eaux De Surface-Eaux Souterraines Dans Un Contexte d'agriculture Irriguée. (Ph.D Thesis). Univ. Liege, 285p.
Hidalgo, M.C., Cruz-Sanjulián, J., Sanroma, A., 1995. Geochemical Evolution of underground waters in a sedimentary river basin (water-bearing of Baza-Caniles, Granada, Spain). Tierra y Technol. 20, 39–48.

Hong, Y.S., Rosen, M.R., 2001. Intelligent characterization and diagnosis of the effect of storm water infiltration on ground water quality in a fractured rock aquifer using artificial neural network. Urban Water 3, 193–204, http://dx.doi.org/10.1016/S1462-0758(01)00045-0.
Hong, S., Kim, H., Kumar, N., Kim, J., Park, N., 2004. Experimental investigations on groundwater flow in coastal aquifers. In: Groundwater and Saline Intrusion., pp. 15, 21p.
Ibrahima, M., Moctar, D., Maguette, D.N., Diakher, M.H., Malick, N.P., Serigne, F., 2015. Evaluation of water resources quality in sabodala gold mining region and its surrounding area (Senegal). J. Water Res. Protect. 7 (3), 247–6363, http://dx.doi.org/10.4236/jwarp.2015.73020.
Jankowski, J., Acworth, R.I., 1997. Impact of debris-flow deposits on hydrogeochemical processes and the development of dry land salinity in the Yass River Catchment, New South Wales. Aust. Hydrogeol. J. 5 (4), 71–88, http://dx.doi.org/10.1007/s100400050119.
Jones, B.F., Vengosh, A., Rosenthal, E., Yechieli, Y., 1999. Geochemical investigations. In: Seawater Intrusion in Coastal Aquifers-Concepts, Methods and Practices. Springer Netherlands. 14, 51–71. 10.1007/978-94-017-2969-7_3.
Kim, Y., Lee, K.S., Koh, D.C., Lee, D.H., Lee, S.G., Park, W.B., Koh, G.W., Woo, N.C., 2003. Hydrogeochemical and isotopic evidence of groundwater salinization in coastal aquifer: a case study in Jeju volcanic island. J. Hydrol. 270 (3), 282–294, http://dx.doi.org/10.1016/S0022-1694(02)00307-4.
Kohonen, T., 1982. Self-organized formation of topologically correct feature maps. Biol.Cybern 43 (1), http://dx.doi.org/10.1007/BF00337288.
Kohonen, T., 2001. An Overview of SOM Literature. In Self-Organizing Maps Springer Berlin Heidelberg. 30, 347–371. 10.1007/978-3-642-56927-2_10.
Koussoube, Y., 2010. Hydrogéologie des séries sédimentaires de la dépression piézométrique du Gondo (bassin du Sourou) – Burkina Faso/Mali. (Ph.D thesis). Paris VI – Pierre et Marie Curie Univ. 285p.
Kristensen, E., Holmer, M., Bussarawit, N., 1991. Benthic metabolism and sulfate reduction in a South-East Asian mangrove swamp. Mar. Ecol. Prog. Ser. 73, 93–103.
Lappartient, J.R., 1985. The Continental Terminal and the Early Pleistocene of the Senegalo-mauritanian Basin. Stratigraphy, Sedimentology, Diagenesis, Alterations, Paleoshore Reconstitutions from the Ferralitic Formations, (PhD Thesis). Univ. Marseille, France, 294p.
Largier, J.L., Smith, S.V., Hollibaugh, J.T., 1997. Seasonally hypersaline estuaries in Mediterranean-climateregions. Est. Coast. Shelf Sci. 45 (6), 789–797, http://dx.doi.org/10.1006/ecss.1997.0279.
Le Priol J., Dieng B., 1985. Synthèse hydrogéologique du Sénégal (1984–1985). Etude géologique structurale par photo-interprétation. Géométrie et limites des aquifères souterrains. Rap. Min. Hydraul. 0l/85fMHIDEH.
Lebel, T., Ali, A., 2009. Recent trends in the Central and Western Sahel rainfall regime (1990–2007). J. Hydrol. 375 (1–2), 52–64, http://dx.doi.org/10.1016/j.jhydrol.2008.11.030.
Lebigre, J.M., Marius, C., 1984. Etude d'une séquence mangrove-tanne en milieu équatorial, baie de la Mondah (Gabon). Photo Ann. Trav. Doc. Géogr. Trop. CGET, 131–145.
Ly, A., Aglanda, R., 1991. Le bassin sénégalo-mauritanien dans l'évolution des marges périatlantique au Tertiaire. Cah. Micropaléontol. 6 (2), 47p.
Magaritz, M., Nadler, A., Koyumdjiski, H., Dan, J., 1981. The use of Na/Cl ratios to trace solute sources in a semiarid zone. Water Resour. Res. 17 (3), 602–608.
Mercado, A., 1985. The use of hydrogeochemical patterns in carbonate sand and sandstone aquifers to identify intrusion and flushing of saline water. Ground Water 23, 635–645, http://dx.doi.org/10.1111/j.1745-6584.1985.tb01512.x.
Mikhailov, V.N., Isupova, M.V., 2008. Hypersalinization of river estuaries in West Africa. Water Resour. 35 (4), 367–385, http://dx.doi.org/10.1134/S0097807808040015.
Montcoudiol, N., Molson, J., Lemieux, J.M., 2015. Groundwater geochemistry of the Outaouais Region (Québec, canada): a regional-scale study. Hydrogeol. J. 23 (2), 337–396.
Mudry, J., 1991. Discriminant analysis an efficient means for the validation geohydrological hypothesis. Rev. Sci. Eau. 4 (1), 19–37, http://dx.doi.org/10.7202/705088ar.
Ndiaye B., Aranyossy J.F., Faye A., 1993. Le rôle de l'évaporation dans la formation des dépressions piézométriques en Afrique Sahélienne; hypothèses et modélisation. In: Les ressources en eau au Sahel. Etudes hydrogéologiques et hydrologiques en Afrique de l'Ouest par les techniques isotopiques, IAEA-TECDOC-721:53-63.
Ngom, F.D., 2000. Caractérisation Des Transferts Hydriques Dans Le Bassin De La Nema Au Sine Saloum. These 3eme Cycle. Univ. Dakar, 130p.
Ngounou Ngatcha, B., Mudry, J., Aranyossy, J.F., Naah, E., Reynault, S.J., 2007. Apport de la géologie, de l'hydrogéologie et des isotopes de l'environnement à la connaissance des nappes en creux″ du Grand Yaéré (Nord Caméroun). Rev. Sci. Eau. 20 (1), 29–43.
Nicolini, E., Rogers, K., Rakowski, D., 2016. Baseline geochemical characterisation of a vulnerable tropical karstic aquifer; Lifou, New Caledonia. J. Hydrol.: Reg. Stud. 5, 114–130.
Noël, Y., 1975. Etude Hydrogéologique Du Continental Terminal De Sine Gambie Première Phase Et Rapport De Synthèse. BRGM Dakar, 30p.
Page, J., Citeau, J., 1990. Rainfall and salinity of a Sahelian estuary between 1927 and 1987. J. Hydrol. 113 (1–4), 325–341, http://dx.doi.org/10.1016/0022-1694(90)90182-w.
Peeters, L., Baçao, F., Lobo, V., Dassargues, A., 2007. Exploratory data analysis and clustering of multivariate spatial hydrogeological data by means of GEO3DSOM, a variant of Kohonen's Self-Organizing Map. Hydrol. Earth Syst. Sci. 11 (4), 1309–1321, http://dx.doi.org/10.5194/hess-11-1309-2007.
Piper, A.M., 1944. A graphical procedure in the geochemical interpretation of water analyses. Trans. Am. Geophys. Union 25 (6), http://dx.doi.org/10.1029/TR025i006p00914.
Pritchard, D.W., 1967. What is an Estuary: Physical Viewpoint. In Lauff, G.H. (Ed.) Estuaries. Am. Ass. Advanc. Sci Pub. 83, 3–5.
Ridd, P.V., Stieglitz, T., 2002. Dry season salinity changes in arid estuaries fringed by mangrovesandsaltflats. Estuar. Coast. Shelf. Sci. 54 (6), 1039–1049, http://dx.doi.org/10.1006/ecss.2001.0876.
Roger, J., Barusseau, J.P., Castaigne, P., Duvail, C., Noël, B.J., Nehlig, P., Serrano, O., Banton, O., Comte, J.C., Travi, Y., Sarr, R., Dabo, B., Diagne, E., Sagna, R., 2009. Programme d'Appui Au Secteur Minier Cartographie géologique Du Bassin sédimentaire. Projet 9 ACP SE 009.
Sarr, R., 1995. Etude biostratigraphique et paléoenvironnementale des séries d'âge Crétacé Terminal à Eocène moyen du Sénégal occidental. In: Systématique Et Migration Des Ostracodes. (Thèse d'Etat). Univ. C.A.D. Dakar, 335p.
Savenije, H., Pagès, J., 1992. Hypersalinity: a dramatic change in the hydrology of Sahelian estuaries. J. Hydrol. 135, 157–174.
Shahul Hameed, A., Resmi, T.R., Suraj, S., Unnikrishnan Warrier, C., Sudheesh, M., Deshpande, R.D., 2015. Isotopic characterization and mass balance reveals groundwater recharge pattern in Chaliyar River basin, Kerala, India. J. Hydrol.: Reg. Stud. 4(A, 48–58.
Smith, A.J., Turner, J.V., 2001. Density-dependent surface water-groundwater interaction and nutrient discharge in the Swan – Canning estuary. Hydrolog. Process. 15 (13), 2595–2616, http://dx.doi.org/10.1002/hyp.303.
Travi, Y., Gac, J.Y., Fontes, J.C., Fritz, B., 1987. Chemical and isotopic survey of rain waters in Senegal. Geodyn 2 (1), 43–53.
Travi, Y., 1988. Hydrogéochimie Et Hydrogéologie Des Aquifères Fluorés Du Bassin Du Sénégal. Origine Et Conditions De Transport Du Fluor Dans Les Eaux Souterraines. Thesis Sci. Univ. Paris Sud (Orsay), 190p.
Vengosh, A., Spivack, A.J., Artzi, Y., Ayalon, A., 1999. Geochemical and boron, strontium, and oxygen isotopic constraints on the origin of the salinity in groundwater from the Mediterranean soast of Israel. Water Resour. Res. 3 (6), 1877–1894, http://dx.doi.org/10.1029/1999WR900024.
Vengosh, A., 2013. Salinization and Saline Environments. In: Sherwood Lollar, B. (Ed.), Environmental geochemistry, Treatise in Geochemistry. Second Ed. 11, 325–378. 10.1016/B978-0-08-095975-7. 00909-8. (Chapter 9 Salinization Treatise in Geochemistry).
WHO, 2008. Guidelines for Drinking-Water Quality, third ed. 1. Recommendations, World Health Organization (WHO), Geneva, Switzerland, 515pp.
Werner A.D., Lockington D.A., 2004. Dynamic groundwater and salt transport near a tidal, partially penetrating estuary. In: Miller C.T., Pinder G.F. (Eds). Computational methods in water resources. 55 (2), 1535–1547. 10.1016/S0167-5648(04)80164-3.
Wolanski, E., 1986. An evaporation-driven salinity maximum zone in Australian tropical estuaries. Estuar. Coast. Mar. Sci. 22 (4), 415–424, http://dx.doi.org/10.1016/0272-7714(86)90065-X.